Journal of Engineering Mathematics **48:** 105–128, 2004.

Quarter-plane problem of a floating elastic plate

KEN TAKAGI
Department of Naval Architecture and Ocean Engineering, Osaka University 2-1 Yamadaoka, Suita, Osaka, 565-0871, Japan (E-mail takagi@naoe.eng.osaka-u.ac.jp)

Received 13 January 2003; accepted in revised form 15 May 2003

Abstract. An investigation is made into the hydro-elastic behavior of a floating elastic plate, which occupies a quarter plane to infinity and is excited by water waves. A boundary-integral equation based on the Green function for this problem is shown for the case of finite water depth, as well as for the case of shallow water. The solution of the quarter-plane problem is composed of the corner effect and the solution of the half-plane problem. The corner effect is divided into two parts. The first part is the end effect of the forcing term of the integral equation, which is analytically estimated and its asymptotic form is derived. The second part is the local contribution whose asymptotic form is also obtained. The asymptotic form of the corner effect is confirmed by a numerical evaluation.

Key words: asymptotic form, hydroelasticity, quarter-plane problem, very rage floating structure

1. Introduction

A very large floating structure, which will be abbreviated VLFS hereinafter, planned in Japan has a thin-plate configuration of very large horizontal size, and can be modeled as a membrane plate of small bending rigidity floating on the water surface. This modeling leads a new free-surface condition, which governs wave motions in the plate, and makes the analysis of hydroelastic behavior of VLFS simpler. Although this approach has a long history in the field of ice floes, at last some studies have applied it to VLFS, (*e.g.* [1]), instead of the so-called modal analysis that is widely applied for hydroelastic problems in the field of floating structures. Benefit of this approach is not only simplicity of the solution, but also facilitates understanding the hydroelastic behavior of VLFS easily, since it insists that the deflection of the plate is represented by a wave motion in the plate. This point of view is very important at the conceptual design stage, because the detailed analysis of the hydroelastic behavior by numerical computations is too expensive and too time consuming. If the designer of VLFS well understands the hydrodynamic behavior, he or she will decide proper shape and/or dimensions of VLFS in the early stages of the design without expensive computations.

The origin of the approach is found in a textbook written by Stoker [2, pp. 438–449]. In the field of ice floes, this approach has been widely used for the study of elastic deformation of an ice floe in waves. Evans and Davies [3] applied this approach to the band problem in which the ice floe is treated as a thin elastic plate of infinite length while the width of plate is finite. They also employed the shallow-water approximation, which makes the problem very simple since the dispersion relation of waves in the plate has only six roots. This implies that the solution is represented with six terms of closed form. The theory predicts the refraction at the edge of the plate and also the critical angle under which all waves are reflected at the edge and no waves are seen in the plate. It is apparent that the accuracy of the dispersion relation plays an important role on the behavior of waves in the plate.

Fox and Squire [4] presented a closed-form solution of the half-plane problem of finite water depth in which the plate is infinitely spread to the half plane. Meylan and Squire [5] suggested the applicability of the wide-spacing approximation, which is widely used in the field of multi-body interaction problems. When the wide-spacing approximation is applied, the band problem can be reduced to the half-plane problem. Besides the wide-spacing approximation, if one employs the shallow-water approximation, the solution will have only three terms. These three terms are plane progressive waves and two exponentially decaying terms. The half-plane problem plays an important role in the present paper.

It is well known that the closed-form solution is very convenient for understanding the physics of the solution. A similar attempt has been made for several two-dimensional geometries. Meylan and Squire [6] presented a closed-form (eigenfunction expansion) solution for an elastic circular disk, which is a physical model of an ice floe floating on water of finite depth. Zilman and Miloh [7] applied the shallow-water approximation to the same problem and obtained a very simple closed-form solution. The solution is represented by a series of modified Bessel functions in the plate, and by a series of Hankel functions outside the plate, which will be called the water domain hereinafter.

The closed-form solution of the band problem can be utilized for the rectangular-plate problem. The solution is represented as an eigenfunction expansion in the vertical direction and the problem is reduced to the solution of the Helmholtz equation in the horizontal plane. Kim and Ertekin [8] applied this method to analyze the elastic motion of VLFS of rectangular geometry. They solved the Helmholtz equation by means of boundary-integral equation. If the plate is not large, the solution could be obtained as a Fourier-series expansion in the horizontal plane and the first few terms give a good approximation, which is convenient to understand the hydrodynamic behavior of the floating elastic plate. However, applying the Fourier series is not a good idea when the plate is very large, since the influence of a corner may disappear at other corners or far from the corner and, therefore, a large number of components are required for an accurate Fourier representation. In this case, the quarter-plane problem, in which an infinitely large plate occupies a quarter plane, gives a better approximation. This is the motivation why we focus on the quarter-plane problem of a floating elastic plate in this paper.

From an analogy with the wide-spacing approximation, the solution may be represented by a series of Hankel functions far from the corner in the quarter-plane problem. On the contrary, the closed-form solution for a circular disk suggests that the modified Bessel function I_n is suitable for a series representation near the corner, since the Hankel function has a singularity at the origin, although the modified Bessel function I_n does not satisfy the radiation condition. Therefore, it seems difficult to obtain a closed-form solution of the quarter-plane problem. This is the reason why we start by deriving a boundary-integral equation with the Green function, instead of tackling the closed-form solution directly. However, we try to decompose the solution in a simple form to be convenient for understanding the hydroelastic behavior of a floating elastic plate.

In this paper, the hydro-elastic behavior of a floating elastic plate is treated on the basis of isotropic, thin-plate theory for the elastic plate deformation and inviscid, linear theory for the liquid motion. The plate occupies the first quadrant, and rigid modes of the plate are negligible because the plate is infinitely large. In Section 2 the problem is formulated as a scattering problem in terms of a velocity potential. In Section 3 we start by deriving a boundary-integral equation with the Green function, which satisfies the elastic free-surface condition. The Green function is represented by a summation of Hankel functions. Then averaging it in the vertical direction, we obtain the shallow-water approximation of the boundary-integral equation in Section 4. Applying the shallow-water boundary-integral equation to the quarter-plane problem, the quarter-plane problem is formulated in Section 5. The solvability of the quarter-plane problem is also discussed.

The solution of the quarter-plane problem is composed of the solution of the half-plane problem and the corner effect. The corner effect can be divided into two parts. The first one is the end effect of the forcing term, which appears in the integral equation. The second one corresponds to the contribution of the corner effect itself to the integral equation, which will be called the local contribution hereinafter. In order to decompose the solution into simple form, the end effect of the forcing term is estimated in Section 6. The end effect is represented in integral form and, it is asymptotically proportional to the inverse square root of the distance from the corner. The asymptotic form of the overall solution is investigated in Section 7. It is found that the corner effect along both edge is inversely proportional to distance. It is also found that the integral representation of the end effect involves a problem on a certain line on which the stationary-phase method cannot be applied to estimate the asymptotic form. The asymptotic form along this line is also discussed. Finally, a numerical calculation is carried out in Section 8 to confirm the asymptotic behavior of the solution. The main purpose of this work is to obtain the asymptotic results presented in Section 7, and these results may be helpful for understanding the hydroelastic behavior of VLFS.

2. General formulation

A flat floating elastic plate of very small draft d is at the surface of an ocean. Let a Cartesian coordinate system (x, y, z) be attached to the free surface of the water so that z is the vertical coordinate decreasing with depth and equal to zero in the undisturbed free surface and x, z are horizontal coordinates. The plate occupies the domain $x, y \in D_p$, $-d \le z \le 0$, where D_p is identical to the first quadrant.

Since the motion of the fluid is supposed to be inviscid, irrotational and incompressible, the velocity potential Φ satisfying Laplace's equation is introduced. Further assumption is that the velocity potential is harmonic in time with an angular frequency ω and it can be represented as $\Phi(x, y, z, t) = \mathfrak{Re}\left[\phi(x, y, z)\mathrm{e}^{\mathrm{i}\omega t}\right]$. When the amplitude of the incoming waves is very small, all equations may be linearized with respect to the amplitude of the incoming waves. Thin-elastic-plate theory [9, pp. 319–347] gives the equation of the vertical displacement ζ of the plate

$$m\frac{\partial^2\zeta}{\partial t^2} = -D\left(\frac{\partial^2}{\partial x^2} + \frac{\partial^2}{\partial y^2}\right)^2 \zeta - \rho g\zeta - \mathrm{i}\rho\omega\phi(x, y, 0), \tag{1}$$

where m is the mass of unit area of the plate, ρ the density of the water and g the gravitational acceleration. D is the flexural rigidity of the plate given by $D = ET^3/12(1-\nu^2)$, where T is the thickness of the plate, E the equivalent Young's modulus and ν Poisson's ratio. The linearized body boundary condition of the plate is derived from the impermeability under the bottom of the plate

$$\mathrm{i}\omega\zeta = \frac{\partial\phi}{\partial z} \qquad \text{at} \quad z = 0, \tag{2}$$

where the bottom condition is imposed at $z = 0$ instead of $z = -d$, since it is assumed that the draft d is negligible order. This assumption coincides with assuming $\omega^2 d/g \ll 1$. When

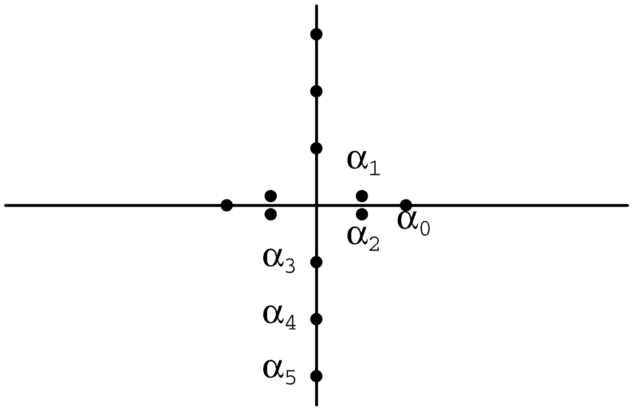

Figure 1. Definition of numbering of the subscript for roots of the dispersion relation (5).

the mass of the plate is uniformly distributed, the local mass of the plate should be balanced by the local buoyancy. Hence, $m = \rho d$ and the left-hand side of (1) is also negligible.

Substituting the body boundary condition of the plate (2) in Equation (1), the free-surface condition is obtained:

$$-K\phi + (1 + M\nabla^4)\frac{\partial \phi}{\partial z} = 0 \qquad \text{at} \quad z = 0, \quad x, y \in D_p, \tag{3}$$

where $K = \omega^2/g$, $M = D/\rho g$, $\nabla^2 = \partial_x^2 + \partial_y^2$. It is assumed that the bottom is horizontal and the depth is h. The following boundary condition is imposed at the bottom of the water.

$$\frac{\partial \phi}{\partial z} = 0 \qquad \text{at} \quad z = -h. \tag{4}$$

Equations (3) and (4) lead to a dispersion relation in the plate with wave number α:

$$K - \alpha(1 + M\alpha^4)\tanh \alpha h = 0. \tag{5}$$

Two roots of (5), $\pm\alpha_0$, are found on the real axis, infinitely many roots $\pm\alpha_n$ $(n = 3, 4\cdots)$ are located on the imaginary axis and four more roots, $\pm\alpha_n$ $(n = 1, 2)$, are found in each quarter plane as shown in Figure 1. A detailed description of the location of the roots is found in [3, pp. 26–28].

When the upper half plane is occupied by a floating elastic plate and plane waves incident perpendicular to the x-axis, the eigenfunction-expansion form of ϕ may be represented by the roots of (5):

$$\phi = T_0 \cosh \alpha_0(z + h)\mathrm{e}^{-\mathrm{i}\alpha_0 y} + T_1 \cosh \alpha_1(z + h)\mathrm{e}^{\mathrm{i}\alpha_1 y} + T_2 \cosh \alpha_2(z + h)\mathrm{e}^{-\mathrm{i}\alpha_2 y} + \sum_{n=3}^{\infty} T_n \cosh \alpha_n(z + h)\mathrm{e}^{-\mathrm{i}\alpha_n y}, \tag{6}$$

where T_n is an unknown constant.

In the water domain, the usual free-surface condition is imposed:

$$-K\phi + \frac{\partial \phi}{\partial z} = 0 \qquad \text{at} \quad z = 0, \quad x, y \in C(D_p), \tag{7}$$

where $C(D_p)$ denotes the water domain.

3. Boundary-integral equation

Applying Green's second identity to the fluid domain covered with the plate and evaluating the integral over the plate by integration by parts, the following boundary-integral equation is obtained

$$\begin{aligned}\phi(x,y,z) = & -\int_c \int_{-h}^{0} \left(\phi \frac{\partial G_d}{\partial n} - \frac{\partial \phi}{\partial n} G_d \right) \mathrm{d}z' \mathrm{d}c \\ & -\frac{M}{K} \int_c \left(\frac{\partial}{\partial z'} (\nabla^2 \phi) \frac{\partial^2 G_d}{\partial n \partial z'} - \frac{\partial^2}{\partial n \partial z'} (\nabla^2 \phi) \frac{\partial G_d}{\partial z'} + \frac{\partial \phi}{\partial z'} \frac{\partial^2}{\partial n \partial z'} (\nabla^2 G_d) \right. \\ & \left. - \frac{\partial^2 \phi}{\partial n \partial z'} \frac{\partial}{\partial z'} (\nabla^2 G_d) \right) \Bigg|_{z'=0} \mathrm{d}c \quad \text{for } x, y \in D_p,\ -h < z < 0, \end{aligned} \tag{8}$$

where c is a integral path which coincides with the edge of the plate and n is normal to the local c-z plane and positive outward from the fluid domain covered with the elastic plate. The Green function satisfies the elastic free-surface condition and the bottom condition, and it is represented as follows:

$$\begin{aligned} & G_d(x,y,z,x',y',z') = \\ & \frac{1}{4\pi}\left(\frac{1}{r} + \frac{1}{r_2}\right) + \frac{1}{2\pi} \lim_{\iota \to 0} \int_0^{\infty} \frac{K + (1 + Mk^4)k}{(K - \mathrm{i}\iota)\cosh kh - (1 + Mk^4)k \sinh kh} \mathrm{e}^{-kh} \times \\ & \times \cosh k(z+h) \cosh k(z'+h) J_0(kR') \mathrm{d}k, \end{aligned} \tag{9}$$

where ι ensures the radiation condition, namely that waves in the plate propagate inward to the plate and

$$r^2 = (x - x')^2 + (y - y')^2 + (z - z')^2, \tag{10}$$

$$r_2^2 = (x - x')^2 + (y - y')^2 + (2h + z + z')^2, \tag{11}$$

$$R'^2 = (x - x')^2 + (y - y')^2. \tag{12}$$

Replacing the Bessel function J_0 in the Green function (9) by Hankel functions of the first and second kinds and applying the contour integral, we can move the integral path on the imaginary axis. If we chose the contours so that the contour for the Hankel function of the first kind is in the first quadrant and the contour for the Hankel function of the second kind is in the fourth quadrant, only the contributions from the poles remain. A similar procedure as applied by John [10] to derive of the series representation of the water-wave Green function of finite depth, yields

$$G_d(x,y,z,x',y',z') = -\frac{\mathrm{i}}{2h}\frac{H_0^{(2)}(\alpha_0 R')\cosh\alpha_0(z+h)\cosh\alpha_0(z'+h)}{1+\dfrac{1+5M\alpha_0^4}{2(1+M\alpha_0^4)\alpha_0 h}\sinh 2\alpha_0 h}$$
$$-\mathfrak{Im}\left[\frac{1}{h}\frac{H_0^{(1)}(\alpha_1 R')\cosh\alpha_1(z+h)\cosh\alpha_1(z'+h)}{1+\dfrac{1+5M\alpha_1^4}{2(1+M\alpha_1^4)\alpha_1 h}\sinh 2\alpha_1 h}\right]$$
$$-\frac{\mathrm{i}}{2h}\sum_{n=3}^{\infty}\frac{H_0^{(2)}(\alpha_n R')\cosh\alpha_n(z+h)\cosh\alpha_n(z'+h)}{1+\dfrac{1+5M\alpha_n^4}{2(1+M\alpha_n^4)\alpha_n h}\sinh 2\alpha_n h}, \tag{13}$$

where $H_0^{(1)}$ and $H_0^{(2)}$ are Hankel functions of the first and second kinds, respectively. The form of the Green function (13) shows that the fourth derivatives of the Green function in the second integral of the integral equation (8) have only a singularity due to the normal derivative of the Hankel function, which does not yield an unbounded velocity potential. Hermans [11] presented a boundary-integral approach to the same problem and derived another type of boundary-integral equation.

At the edge of the plate, the fact that the moment and the shearing force are free leads to the following two conditions; see [3, p. 44].

$$\frac{\partial^3\phi}{\partial n^2\partial z}+\nu\frac{\partial^3\phi}{\partial s^2\partial z}=0,\qquad \nabla^2\frac{\partial^2\phi}{\partial z\partial n}+(1-\nu)\frac{\partial^4\phi}{\partial s^2\partial n\partial z}=0\qquad \text{at}\quad z=0, \tag{14}$$

where s denotes the tangential measure along the edge of the plate. If we solve the boundary-integral equation (8) together with the edge boundary condition (14) and certain forcing term, the deflection of the plate will be obtained.

4. Shallow-water approximation

It is well known that the water-wave problem is greatly simplified by the shallow-water approximation, since all evanescent terms vanish. Employing the shallow-water approximation, we may represent the velocity potential as follows:

$$\phi(x,y,z)\sim\varphi(x,y)-\frac{1}{2}(z+h)^2\,\nabla^2\,\varphi. \tag{15}$$

Substituting (15) in (8), performing integration with respect to z' and eliminating higher-order terms proportional to $O(h^2)$, we find that the boundary-integral equation (8) becomes very simple.

$$\varphi(x,y) = -\int_c\left(\varphi\frac{\partial}{\partial n}-\frac{\partial\varphi}{\partial n}\right)G(x,x',y,y')\mathrm{d}c+M\int_c\left(\nabla^2\varphi\frac{\partial}{\partial n}-\frac{\partial}{\partial n}(\nabla^2\varphi)\right)G_1(x,x',y,y')\mathrm{d}c$$
$$-M\int_c\left(\nabla^4\varphi\frac{\partial}{\partial n}-\frac{\partial}{\partial n}(\nabla^4\varphi)\right)G_2(x,x',y,y')\mathrm{d}c\quad \text{for } x,y\in D_p, \tag{16}$$

where

$$G(x, x', y, y') = \lim_{\iota \to 0} \frac{1}{2\pi} \int_0^\infty \frac{K}{k} \left(\frac{1}{K - \mathrm{i}\iota - (1 + Mk^4)k^2h} - \frac{1}{K - \mathrm{i}\iota} \right) J_0(kR')\mathrm{d}k$$
$$= -\mathrm{i}\frac{KH_0^{(2)}(\alpha_0 R')}{2\alpha_0 \Omega'(\alpha_0)} - \mathfrak{Im}\left[\frac{KH_0^{(1)}(\alpha_1 R')}{\alpha_1 \Omega'(\alpha_1)}\right], \tag{17}$$

$$G_1(x, x', y, y') = \lim_{\iota \to 0} \frac{1}{2\pi} \int_0^\infty \frac{k^3 h}{K - \mathrm{i}\iota - (1 + Mk^4)k^2h} J_0(kR')\mathrm{d}k$$
$$= -\mathrm{i}\frac{\alpha_0^3 h H_0^{(2)}(\alpha_0 R')}{2\Omega'(\alpha_0)} - \mathfrak{Im}\left[\frac{\alpha_1^3 h H_0^{(1)}(\alpha_1 R')}{\Omega'(\alpha_1)}\right], \tag{18}$$

$$G_2(x, x', y, y') = \lim_{\iota \to 0} \frac{1}{2\pi} \int_0^\infty \frac{kh}{K - \mathrm{i}\iota - (1 + Mk^4)k^2h} J_0(kR')\mathrm{d}k$$
$$= -\mathrm{i}\frac{\alpha_0 h H_0^{(2)}(\alpha_0 R')}{2\Omega'(\alpha_0)} - \mathfrak{Im}\left[\frac{\alpha_1 h H_0^{(1)}(\alpha_1 R')}{\Omega'(\alpha_1)}\right], \tag{19}$$

where $\Omega(\alpha) = 0$ denotes the dispersion relation in the shallow-water approximation by defined by

$$\Omega(\alpha) = K - (1 + M\alpha^4)\alpha^2 h. \tag{20}$$

The shallow-water dispersion relation $\Omega(\alpha) = 0$ has two roots on the real axis and four roots in each one of the quadrants. The explanation of the positioning of these roots is found in [3, p. 56].

Equations (17) and (18) can benefit from an observation. When the value M is infinitesimal, then

$$\alpha_1 = \frac{1 + \mathrm{i}}{\sqrt{2}} M^{-1/4} \left(1 + O(M^{1/2})\right). \tag{21}$$

Hence, the strength of the singularity of (17) is $O(M)$ and that of (18) is $O(1)$. This implies that (16) will be identical to the boundary-integral equation for the water domain if the value $M = 0$ is inserted, although the integral equation for the water domain will be obtained by another approach in Section 5.

It is noted that, since higher-order terms proportional to $O(h^2)$ are neglected in the integral equation (16) as mentioned above, all equations are consistent up to $O(h)$, and the two-dimensional velocity potential φ satisfies

$$K\varphi + \left(1 + M\nabla^4\right) \nabla^2 \varphi h = 0. \tag{22}$$

5. Formulation of quarter-plane problem

Suppose a semi-infinite quarter plate which occupies ($x > 0$, $y > 0$) and plane progressive waves coming from the water domain whose angle of direction with x-axis is χ. It is obvious from the radiation condition that the contribution of the boundary at infinity vanishes. Therefore, the path of integration in (16) becomes $x' = 0$ and $y' = 0$:

$$\varphi(x,y) = -\int_0^\infty \left[\left(\varphi\frac{\partial}{\partial y'} - \frac{\partial\varphi}{\partial y'}\right)G(x,x',y,0) - M\left(\nabla^2\varphi\frac{\partial}{\partial y'} - \frac{\partial}{\partial y'}(\nabla^2\varphi)\right)G_1(x,x',y,0) \right.$$
$$\left. + M\left(\nabla^4\varphi\frac{\partial}{\partial y'} - \frac{\partial}{\partial y'}(\nabla^4\varphi)\right)G_2(x,x',y,0)\right]\mathrm{d}x' + \int_0^\infty\left[\left(\varphi\frac{\partial}{\partial x'} - \frac{\partial\varphi}{\partial x'}\right)G(x,0,y,y') \right.$$
$$- M\left(\nabla^2\varphi\frac{\partial}{\partial x'} - \frac{\partial}{\partial x'}(\nabla^2\varphi)\right)G_1(x,0,y,y') \tag{23}$$
$$\left. + M\left(\nabla^4\varphi\frac{\partial}{\partial x'} - \frac{\partial}{\partial x'}(\nabla^4\varphi)\right)G_2(x,0,y,y')\right]\mathrm{d}y' \quad \text{for } x,y \in D_p.$$

The edge conditions become

$$\nabla^4\varphi - (1-\nu)\frac{\partial^2}{\partial x^2}(\nabla^2\varphi) = 0,\ \frac{\partial}{\partial y}(\nabla^4\varphi) + (1-\nu)\frac{\partial^3}{\partial x^2\partial y}(\nabla^2\varphi) = 0 \quad \text{at} \quad y = 0, \tag{24}$$

$$\nabla^4\varphi - (1-\nu)\frac{\partial^2}{\partial y^2}(\nabla^2\varphi) = 0,\ \frac{\partial}{\partial x}(\nabla^4\varphi) + (1-\nu)\frac{\partial^3}{\partial y^2\partial x}(\nabla^2\varphi) = 0 \quad \text{at} \quad x = 0. \tag{25}$$

In addition, a concentrated force stemming from replacement of the torsional moment with an equivalent shear force must be zero at the corner

$$\frac{\partial^2}{\partial x\partial y}(\nabla^2\varphi) = 0 \qquad \text{at} \quad x = y = 0. \tag{26}$$

Applying Green's second identity to the water domain and employing the shallow water approximation, we obtain a similar boundary-integral equation for the outside of the plate ($\{x < 0\} \cup \{y < 0\}$), namely

$$\tilde{\varphi}(x,y) = -\int_0^\infty \left(\tilde{\varphi}\frac{\partial}{\partial y'} - \frac{\partial\tilde{\varphi}}{\partial y'}\right)G_w(x,x',y,0)\mathrm{d}x'$$
$$+ \int_0^\infty \left(\tilde{\varphi}\frac{\partial}{\partial x'} - \frac{\partial\tilde{\varphi}}{\partial x'}\right)G_w(x,0,y,y')\mathrm{d}y' \quad \text{for } x,y \in C(D_p), \tag{27}$$

where

$$G_w(x,x',y,y') = \lim_{\iota\to 0}\frac{1}{2\pi}\int_0^\infty \frac{K}{k}\left(\frac{1}{K - \mathrm{i}\iota - k^2h} - \frac{1}{K - \mathrm{i}\iota}\right)J_0(kR')\mathrm{d}k = \frac{\mathrm{i}}{4}H_0^{(2)}(k_0R') \tag{28}$$

and k_0 denotes the positive root of the usual shallow-water dispersion relation. The velocity potential and the flux must be continuous at the edge

$$\varphi = \tilde{\varphi}, \quad \frac{\partial\varphi}{\partial y} = \frac{\partial\tilde{\varphi}}{\partial y} \qquad \text{at} \quad y = 0, \tag{29}$$

$$\varphi = \tilde{\varphi}, \quad \frac{\partial\varphi}{\partial x} = \frac{\partial\tilde{\varphi}}{\partial x} \qquad \text{at} \quad x = 0. \tag{30}$$

When the shape of the plate is a circle, the solution can be represented in the eigenfunction expansion form as suggested in Section 1. Thus, we try to apply Graf's addition theorem of the Bessel function to decompose the Green functions in (23) and to obtain an eigenfunction-expansion form of this problem. However, it is immediately found that the uniform expansion cannot be obtained in the case of the quarter-plane problem. When the observation point is far from the corner point, the solution must be represented by a series of the Hankel functions. On the other hand, when the observation point is close to the corner, the solution has no singularity and should be represented by a series of the modified Bessel functions I_n. It seems impossible to unify these expansions. Hence, we try to solve the boundary-integral equation (23) directly.

In order to simplify the description of Equation (23), a vector notation is introduced

$$\vec{\varphi} = (\varphi_1, \varphi_2, \varphi_3, \varphi_4, \varphi_5, \varphi_6) \equiv \left(\varphi, \frac{\partial \varphi}{\partial n}, \nabla^2\varphi, \frac{\partial}{\partial n}(\nabla^2\varphi), \nabla^4\varphi, \frac{\partial}{\partial n}(\nabla^4\varphi)\right). \tag{31}$$

The component of this vector along the lines $x = 0$ or $y = 0$ coincides with unknowns in the integral equation (23). A function $F_p(\vec{\varphi})$ is defined

$$\begin{aligned} F_p(\vec{\varphi}) \equiv\ &-\int_0^\infty \left[\left(\varphi_1(x',0)\frac{\partial}{\partial y'} - \varphi_2(x',0)\right) G(x,x',y,0)\right.\\ &-M\left(\varphi_3(x',0)\frac{\partial}{\partial y'} - \varphi_4(x',0)\right) G_1(x,x',y,0)\\ &\left.+M\left(\varphi_5(x',0)\frac{\partial}{\partial y'} - \varphi_6(x',0)\right) G_2(x,x',y,0)\right]\mathrm{d}x'\\ &+\int_0^\infty \left[\left(\varphi_1(0,y')\frac{\partial}{\partial x'} - \varphi_2(0,y')\right) G(x,0,y,y')\right.\\ &-M\left(\varphi_3(0,y')\frac{\partial}{\partial x'} - \varphi_4(0,y')\right) G_1(x,0,y,y')\\ &\left.+M\left(\varphi_5(0,y')\frac{\partial}{\partial x'} - \varphi_6(0,y')\right) G_2(x,0,y,y')\right]\mathrm{d}y'. \end{aligned} \tag{32}$$

It is noted that differentiation with respect to n in the components φ_2, φ_4 and φ_6 represents differentiation with respect to x or y along the edge $y = 0$ or $x = 0$, respectively, in the integral equation (32). However, for the sake of simplicity, we use the same notation $\partial/\partial n$ in (31).

Similarly, the function $F_w(\vec{\varphi})$ is defined to simplify the representation of integral equation (27)

$$\begin{aligned} F_w(\vec{\varphi}) \equiv\ &-\int_0^\infty \left(\varphi_1(x',0)\frac{\partial}{\partial y'} - \varphi_2(x',0)\right) G_w(x,x',y,0)\mathrm{d}x'\\ &+\int_0^\infty \left(\varphi_1(0,y')\frac{\partial}{\partial x'} - \varphi_2(0,y')\right) G_w(x,0,y,y')\mathrm{d}y', \end{aligned} \tag{33}$$

where the continuity conditions (29) and (30) are implicitly satisfied. Equations (23) and (27) are simply represented as follows:

$$\varphi_1(x,y) = F_p(\vec{\varphi}) \quad \text{for } x, y \in D_p, \tag{34}$$

$$\varphi_1(x,y) = F_w(\vec{\varphi}) \quad \text{for } x, y \in C(D_p). \tag{35}$$

Since (22) includes the sixth derivative of the velocity potential φ, we obtain other two independent integral equations

$$\varphi_3(x,y) = \nabla^2 F_p(\vec{\varphi}) \quad \text{for } x,y \in D_p, \tag{36}$$

$$\varphi_5(x,y) = \nabla^4 F_p(\vec{\varphi}) \quad \text{for } x,y \in D_p. \tag{37}$$

The edge conditions give two further equations

$$\varphi_5 - (1-\nu)\frac{\partial^2 \varphi_3}{\partial s^2} = 0 \qquad \text{for} \quad x = 0 \quad \text{or} \quad y = 0, \tag{38}$$

$$\varphi_6 + (1-\nu)\frac{\partial^2 \varphi_4}{\partial s^2} = 0 \qquad \text{for} \quad x = 0 \quad \text{or} \quad y = 0. \tag{39}$$

After appropriate discretization, these six equations become a system of linear equations. Thus, we can obtain the solution; however, the forcing term does not explicitly appear in this system of linear equations.

When the plate is infinitely large and occupies the upper half plane, the solution is easily obtained by a classical method. This problem is called the upper-half-plane problem hereinafter. Similarly, when the right half plane is occupied by the plate, the solution is also easily obtained. This problem is called the right-half-plane problem hereinafter.

The velocity potential of the upper-half-plane problem $\varphi_{U1}^{(1)}$ is assumed to be composed of two-dimensional waves in the plate with certain wave numbers

$$\varphi_{U1}^{(1)} = \sum_{n=0}^{2} A_n \mathrm{e}^{-\mathrm{i}\alpha_n (x\cos\mu_{xn} + y\sin\mu_{xn})} \qquad \text{for} \quad y > 0, \tag{40}$$

where A_n is a constant value and μ_{xn} denotes the direction of wave propagation in the plate; it has the following relation with the direction χ of the incident waves

$$\alpha_n \cos\mu_{xn} = k_x = k_0 \cos\chi. \tag{41}$$

The velocity potential of the right-half-plane problem $\varphi_{R1}^{(1)}$ is represented as follows:

$$\varphi_{R1}^{(1)} = \sum_{n=0}^{2} C_n \mathrm{e}^{-\mathrm{i}\alpha_n (x\cos\mu_{yn} + y\sin\mu_{yn})} \qquad \text{for} \quad x > 0, \tag{42}$$

where C_n is a constant value and μ_{yn} denotes the direction of wave propagation in the plate; it has the following relation with the direction χ of the incident waves

$$\alpha_n \sin\mu_{yn} = k_y = k_0 \sin\chi. \tag{43}$$

It is noted that μ_{y0} is not a real value and $\mathfrak{Re}[\mu_{y0}] = \frac{\pi}{2}$, because it is assumed, for the simplicity of the analysis, that the angle of incidence χ is smaller than the critical angle.

In order to separate the forcing term, the vector $\vec{\varphi}$ is divided into two parts $\vec{\varphi}^{(1)}$ and $\vec{\varphi}^{(2)}$. It is defined that the velocity potential of the first part $\varphi_1^{(1)}$, *i.e.*, the first component of $\vec{\varphi}^{(1)}$, is the sum of the upper-half-plane problem $\varphi_{U1}^{(1)}$ and the right-half-plane problem $\varphi_{R1}^{(1)}$

$$\varphi_1^{(1)} \equiv \varphi_{U1}^{(1)} + \varphi_{R1}^{(1)} = \sum_{n=0}^{2} \left\{ A_n \mathrm{e}^{-i\alpha_n (x\cos\mu_{xn} + y\sin\mu_{xn})} + C_n \mathrm{e}^{-\mathrm{i}\alpha_n (x\cos\mu_{yn} + y\sin\mu_{yn})} \right\}. \tag{44}$$

It is assumed that $\varphi_1^{(1)}$ coincides with the solution of the quarter-plane problem when the observation point is far from the corner along both edges of the plate. In order to equalize $\varphi_1^{(1)}$ to the plane-wave terms C_{I1}, C_{I2} and C_{I3} appearing in the forcing term (which will be explained in Section 6), additional constraints are imposed:

$$A_0 = 0 \quad \text{when } \frac{\pi}{2} > \arctan\frac{y}{x} > \mu_{x0}, \tag{45}$$

$$A_2 = 0 \quad \text{when } \frac{\pi}{2} > \arctan\frac{y}{x} > \mathfrak{Re}[\mu_{x2}]. \tag{46}$$

It is noted that, because of these constraints, $\varphi_1^{(1)}$ is discontinuous. The constants A_n and C_n are evaluated by some simple algebra outlined in Appendix A. Other components of $\vec{\varphi}^{(1)}$ are obtained by differentiating $\varphi_1^{(1)}$.

The second part $\vec{\varphi}^{(2)}$ represents the corner effect. Substituting this notation, the system of equations is altered

$$\varphi_1^{(2)} - F_w(\vec{\varphi}^{(2)}) = -\varphi_1^{(1)} + F_w(\vec{\varphi}^{(1)}), \tag{47}$$

$$\varphi_1^{(2)} - F_p(\vec{\varphi}^{(2)}) = -\varphi_1^{(1)} + F_p(\vec{\varphi}^{(1)}), \tag{48}$$

$$\varphi_3^{(2)} - \nabla^2 F_p(\vec{\varphi}^{(2)}) = -\varphi_3^{(1)} + \nabla^2 F_p(\vec{\varphi}^{(1)}), \tag{49}$$

$$\varphi_5^{(2)} - \nabla^4 F_p(\vec{\varphi}^{(2)}) = -\varphi_5^{(1)} + \nabla^4 F_p(\vec{\varphi}^{(1)}), \tag{50}$$

$$\varphi_5^{(2)} - (1-\nu)\frac{\partial^2}{\partial s^2}\varphi_3^{(2)} = 0, \tag{51}$$

$$\varphi_6^{(2)} + (1-\nu)\frac{\partial^2}{\partial s^2}\varphi_4^{(2)} = 0, \tag{52}$$

for $\quad x = 0 \quad$ or $\quad y = 0$.

In this system of linear equations, the right-hand side is the forcing term.

6. Forcing term

We try to evaluate the forcing term of Equations (47–50) for the first step. Since the solution of the half plane problem is sinusoidal along the boundary, the following integral is evaluated.

$$\begin{aligned} I &= \lim_{\epsilon\to 0}\int_0^\infty \mathrm{e}^{-\mathrm{i}(k_x-\mathrm{i}\epsilon)x'} G(x,x',y,0)\mathrm{d}x' \qquad (53)\\ &= \lim_{\epsilon,\iota\to 0}\frac{1}{2\pi}\int_0^\infty \mathrm{e}^{-\mathrm{i}(k_x-\mathrm{i}\epsilon)x'} \times \int_0^\infty \frac{K}{k}\left(\frac{1}{K-\mathrm{i}\iota-(1+Mk^4)k^2h} - \frac{1}{K-\mathrm{i}\iota}\right) J_0(kR')\mathrm{d}k\mathrm{d}x', \end{aligned}$$

where ϵ determines positions of the poles appearing in (B2) and k_x denotes the x-component of the wave number of incident waves in the water domain. It is noted that all forcing terms appearing in (47–50) are evaluated by a similar integral without essential difference. Thus, in order to avoid the lengthy expression, we focused on this integral as a typical forcing term.

Applying a contour integral to (53), we can derive a component of plane waves. The details of the derivation are presented in Appendix B.

$$I = -\frac{\mathrm{i}}{2\pi}\frac{K}{\alpha_0\Omega'(\alpha_0)}\int_{-\infty}^{\infty}\frac{\mathrm{e}^{-\mathrm{i}\alpha_0 R\cosh\theta}}{k_x-\alpha_0\cos(\beta+\mathrm{i}\theta)}\mathrm{d}\theta - \frac{i}{2\pi}\frac{K}{\alpha_1\Omega'(\alpha_1)}\int_{-\infty}^{\infty}\frac{\mathrm{e}^{\mathrm{i}\alpha_1 R\cosh\theta}}{k_x+\alpha_1\cos(\beta+\mathrm{i}\theta)}\mathrm{d}\theta$$
$$-\frac{\mathrm{i}}{2\pi}\frac{K}{\alpha_2\Omega'(\alpha_2)}\int_{-\infty}^{\infty}\frac{\mathrm{e}^{-\mathrm{i}\alpha_2 R\cosh\theta}}{k_x-\alpha_2\cos(\beta+\mathrm{i}\theta)}\mathrm{d}\theta + C_{I1}+C_{I2}+C_{I3}, \tag{54}$$

where

$$C_{I1} = \begin{cases} 0 & \text{when } \frac{\pi}{2} > \beta > \mu_{x0} \\ -\mathrm{i}\dfrac{K\mathrm{e}^{-\mathrm{i}R\alpha_0\cos(\mu_{x0}-\beta)}}{\alpha_0^2\Omega'(\alpha_0)\sin\mu_{x0}} & \text{when } 0 < \beta < \mu_{x0} \end{cases}, \tag{55}$$

$$C_{I2} = -\mathrm{i}\frac{K e^{\mathrm{i}R\alpha_1\cos(\mu_{x1}-\beta)}}{\alpha_1^2\Omega'(\alpha_1)\sin\mu_{x1}}, \tag{56}$$

$$C_{I3} = \begin{cases} 0 & \text{when } \frac{\pi}{2} > \beta > \mathfrak{Re}[\mu_{x2}] \\ -\mathrm{i}\dfrac{K\mathrm{e}^{-\mathrm{i}R\alpha_2\cos(\mu_{x2}-\beta)}}{\alpha_2^2\Omega'(\alpha_2)\sin\mu_{x2}} & \text{when } 0 < \beta < \mathfrak{Re}[\mu_{x2}] \end{cases}, \tag{57}$$

$$R = \sqrt{x^2+y^2}, \qquad \beta = \arctan\frac{y}{x}. \tag{58}$$

It is noted that C_{I1} denotes plane progressive waves and it does not decay, since α_0 is a real number. C_{I2} and C_{I3} are also plane progressive waves; however, their wave number is complex and these waves decay quickly as the coordinate y becomes large. The first three terms in (54) represent the end effect of the forcing term and the first term is asymptotically proportional to $1/\sqrt{R}$. When the observation point is far from the corner, the end effect vanishes and the solution coincides with the solution of the semi-infinite half-plane problem. A similar result is also obtained in the water domain:

$$W = \lim_{\epsilon\to 0}\int_0^{\infty}\mathrm{e}^{-\mathrm{i}(k_x-\mathrm{i}\epsilon)x'}G_w(x,x',y,0)\mathrm{d}x' = -\frac{\mathrm{i}}{4\pi}\int_{-\infty}^{\infty}\frac{\mathrm{e}^{-\mathrm{i}k_0 R\cosh\theta}}{k_x-k_0\cos(\beta+\mathrm{i}\theta)}\mathrm{d}\theta + C_{W1}, \tag{59}$$

where

$$C_{W1} = \begin{cases} 0 & \text{when } -\dfrac{3}{2}\pi < \beta < -\chi \\ \mathrm{i}\dfrac{\mathrm{e}^{-\mathrm{i}Rk_0\cos(\chi+\beta)}}{2k_0\sin\chi} & \text{when } 0 > \beta > -\chi \end{cases}. \tag{60, 61}$$

It is noted that the solution of the half-plane problem satisfies the integral equations (32) and (33) when the observation point is far from the corner. Therefore, only the end effect remains as the forcing term in (47–50).

7. Asymptotic form of the solution

The forcing terms of (47) and (48) are represented in the asymptotic form with constants A_0 and C_0, as follows

$$-\varphi_1^{(1)} + F_w(\vec{\varphi}^{(1)}) \sim \frac{e^{-ik_0R - i\frac{\pi}{4}}}{\sqrt{\pi k_0 R}} \left(\frac{\sin\beta - \sin\chi}{k_x - k_0\cos\beta} A_0 + \frac{\cos\beta - \cos\chi}{k_y - k_0\sin\beta} C_0 \right), \tag{62}$$

$$-\varphi_1^{(1)} + F_p(\vec{\varphi}^{(1)}) \sim \frac{e^{-i\alpha_0R - i\frac{\pi}{4}}}{\sqrt{\pi \alpha_0 R}} \left(\frac{\sin\beta + \sin\mu_{x0}}{k_x - \alpha_0\cos\beta} A_0 + \frac{\cos\beta + \cos\mu_{y0}}{k_y - \alpha_0\sin\beta} C_0 \right). \tag{63}$$

The derivation of the asymptotic form is described in Appendix B.

Since the forcing terms are asymptotically proportional to $1/\sqrt{R}$, the vector potential $\vec{\varphi}^{(2)}$ is supposed to contain components which are asymptotically proportional to $1/\sqrt{R}$. It is defined that all these terms are represented by $\vec{\varphi}_R$ and the remainder represented by $\vec{\varphi}_L$. Thus, $\vec{\varphi}_L$ decays more quickly than $1/\sqrt{R}$ as $R \to \infty$. Then $\vec{\varphi}^{(2)}$ has the form

$$\vec{\varphi}^{(2)} = \vec{\varphi}_R + \vec{\varphi}_L \qquad \text{when} \quad R \to \infty. \tag{64}$$

Substituting the vector potential $\vec{\varphi}^{(2)}$ in (23), the contribution of $\vec{\varphi}^{(2)}$ to the boundary-integral equation is obtained. It is apparent that the contribution of $\vec{\varphi}_L$ has the following asymptotic form because of the nature of the Green function:

$$F_p(\vec{\varphi}_L) \sim \vec{L}^{(\alpha)}(\beta)\frac{e^{-i\alpha_0 R}}{\sqrt{R}} \qquad \text{when} \quad 0 < \beta < \frac{\pi}{2}, \tag{65}$$

$$F_w(\vec{\varphi}_L) \sim \vec{L}^{(k)}(\beta)\frac{e^{-ik_0 R}}{\sqrt{R}} \qquad \text{when} \quad -\frac{3}{2}\pi < \beta < 0, \tag{66}$$

where $\vec{L}^{(\alpha)}(\beta)$ and $\vec{L}^{(k)}(\beta)$ are functions of β. Next, we try to evaluate the contribution of $\vec{\varphi}_R$ to the integral equation. The details are shown in Appendix C.

Now we know the asymptotic form of the velocity potential at the infinity. Equations (65), (C11) and (C12) shows that $\vec{\varphi}_R$ is composed of the following five components

$$\begin{aligned}
\vec{\varphi}_R(x,y) \sim\ & \vec{\sigma}^{(\alpha)}(\beta)\frac{e^{-i\alpha_0 R}}{\sqrt{R}} + C_x^{(\alpha)}\left(\vec{\sigma}_{x1}^{(\alpha)}\frac{e^{-i\alpha_0 x + iy\sqrt{\alpha_1^2-\alpha_0^2}}}{\sqrt{x}} + \vec{\sigma}_{x2}^{(\alpha)}\frac{e^{-i\alpha_0 x + iy\sqrt{\alpha_2^2-\alpha_0^2}}}{\sqrt{x}}\right) \\
& + C_y^{(\alpha)}\left(\vec{\sigma}_{y1}^{(\alpha)}\frac{e^{ix\sqrt{\alpha_1^2-\alpha_0^2} - i\alpha_0 y}}{\sqrt{y}} + \vec{\sigma}_{y2}^{(k)}\frac{e^{ix\sqrt{\alpha_2^2-\alpha_0^2} - i\alpha_0 y}}{\sqrt{y}}\right) \\
& + C_x^{(k)}\left(\vec{\sigma}_{x1}^{(k)}\frac{e^{-ik_0 x + iy\sqrt{\alpha_1^2-k_0^2}}}{\sqrt{x}} + \vec{\sigma}_{x2}^{(k)}\frac{e^{-ik_0 x + iy\sqrt{\alpha_2^2-k_0^2}}}{\sqrt{x}}\right) \\
& + C_x^{(k)}\left(\vec{\sigma}_{y1}^{(k)}\frac{e^{ix\sqrt{\alpha_1^2-k_0^2} - ik_0 y}}{\sqrt{y}} + \vec{\sigma}_{y2}^{(k)}\frac{e^{ix\sqrt{\alpha_2^2-k_0^2} - ik_0 y}}{\sqrt{y}}\right),
\end{aligned} \tag{67}$$

where $\vec{\sigma}^{(\alpha)}(\beta)$ is a function of β, and $C_x^{(\alpha)}$, $C_y^{(\alpha)}$, $C_x^{(k)}$ and $C_y^{(k)}$ are constants. The coefficients $\vec{\sigma}_{x1}^{(\alpha)}, \vec{\sigma}_{x2}^{(\alpha)}, \vec{\sigma}_{y1}^{(\alpha)}, \vec{\sigma}_{y2}^{(\alpha)}, \vec{\sigma}_{x1}^{(k)}, \vec{\sigma}_{x2}^{(k)}, \vec{\sigma}_{y1}^{(k)}$ and $\vec{\sigma}_{y2}^{(k)}$ are obtained by Equations (C11) and (C12), but are too lengthy to present here.

Substituting (67) in Equations (51) and (52) and extracting four groups, which are proportional to $e^{-ix\alpha_0}/\sqrt{x}$, $e^{-iy\alpha_0}/\sqrt{y}$, $e^{-ixk_0}/\sqrt{x}$ and $e^{-iyk_0}/\sqrt{y}$, respectively, it is found that $\vec{\sigma}^{(\alpha)}(0)$, $\vec{\sigma}^{(\alpha)}(\frac{\pi}{2})$, $C_x^{(\alpha)}$, $C_y^{(\alpha)}$, $C_x^{(k)}$ and $C_y^{(k)}$ should be zero.

Similarly, $\vec{\varphi}_R$ in the water domain has the following form as shown in Appendix C

$$\vec{\varphi}_R(x,y) \sim \vec{\sigma}^{(k)}(\beta)\frac{\mathrm{e}^{-\mathrm{i}k_0 R}}{\sqrt{R}} + \begin{cases} \vec{\sigma}_x^{(\alpha)} \dfrac{\mathrm{e}^{-\mathrm{i}\alpha_0 x + \mathrm{i}y\sqrt{k_0^2-\alpha_0^2}}}{\sqrt{x + y\dfrac{\alpha_0}{\sqrt{k_0^2-\alpha_0^2}}}} & \text{when } -\beta_c < \beta < 0, \\ 0 & \text{when } -\frac{3}{2}\pi + \beta_c < \beta < -\beta_c, \\ \vec{\sigma}_y^{(\alpha)} \dfrac{\mathrm{e}^{\mathrm{i}x\sqrt{k_0^2-\alpha_0^2} - \mathrm{i}\alpha_0 y}}{\sqrt{x\dfrac{\alpha_0}{\sqrt{k_0^2-\alpha_0^2}} + y}} & \text{when } -\frac{3}{2}\pi < \beta < -\frac{3}{2}\pi + \beta_c, \end{cases} \tag{68}$$

where $\vec{\sigma}^{(k)}(\beta)$ is a function of β and, $\vec{\sigma}_x^{(\alpha)}$ and $\vec{\sigma}_y^{(\alpha)}$ are constant vectors. However, the continuity conditions of the velocity potential and the normal velocity suggest that $\vec{\sigma}^{(k)}(0) = \vec{\sigma}^{(k)}(\frac{\pi}{2}) = 0$ and $\vec{\sigma}_x^{(\alpha)} = \vec{\sigma}_y^{(\alpha)} = 0$. Thus, it is found that the corner effect along the x-axis and the y-axis decays more rapidly than $1/\sqrt{R}$ at infinity, *i.e.*, $\vec{\varphi}_R$ vanishes at both the edges.

The asymptotic form of the end effect of the forcing term in the plate is represented in (63) as mentioned previously, but a problem appears when β approaches to μ_{x0}. When β is equal to μ_{x0}, the denominator of the asymptotic form becomes zero. In this case, the stationary-phase method is not suitable for obtaining the asymptotic form.

Takagi [12] discussed the applicability of the parabolic approximation to this problem and found that the asymptotic form along this line is represented by an anti-symmetric type of parabolic approximation, which can be found in a text book by Mei [13, pp. 486–491] as an approximation of the wave elevation behind a break water. According to this theory, we get the asymptotic form along the line $\beta = \mu_{x0}$ after a suitable modification of the coordinate system

$$I \sim \frac{\mathrm{i}-1}{2}\frac{K\mathrm{e}^{-\mathrm{i}\alpha_0 R\cos(\beta-\mu_{x0})}}{\alpha_0^2\Omega'(\alpha_0)}\left[\frac{1}{2} + C(\sigma) - \mathrm{i}\left(\frac{1}{2} + S(\sigma)\right)\right], \tag{69}$$

where $\sigma = \sqrt{\alpha_0 R}\sin(\beta - \mu_{x0})/\sqrt{\pi\cos(\beta - \mu_{x0})}$ and $C(\sigma)$ and $S(\sigma)$ are the Fresnel cosine and sine integrals. Equation (69) shows that the decay of I becomes slower and slower as β approaches μ_{x0}; however the I decays proportionally to $1/\sqrt{R}$ in general, and finally I does not decay anymore just on the line $\beta = \mu_{x0}$. On the other hand, $\vec{\varphi}_L$ presents no difficulties on this line.

Summarizing the results, the asymptotic form of the quarter plane problem coincides with the solution of the half-plane problem far from the corner and the anti-symmetric-type parabolic approximation presents the asymptotic form near the line $\beta = \mu_{x0}$. If one moves the observation point closer to the corner, all other terms should be taken into account, since these terms are asymptotically proportional to $1/\sqrt{R}$. On both edges, these terms are still negligible, since they decay more rapidly than $1/\sqrt{R}$, *i.e.*, they may be proportional to $1/R$ as demonstrated numerically in Section 8. This summary is violated when μ_{x0} approaches the x-axis or y-axis. This case is analyzed by Takagi [12].

8. Numerical evaluation

In order to confirm the asymptotic form of the solution, it is numerically investigated in this section. The numerical scheme used here is the so-called constant panel method for the discretization of the boundary-integral equations (32) and (33) and the central-difference scheme for the discretization of the edge conditions (51) and (52). At the corner, the central-difference scheme for the second-order derivative in the edge condition requires a virtual node in the water domain. The values of $\varphi_3^{(2)}$ and $\varphi_4^{(2)}$ at the virtual node are determined from the corner condition (26). The details of this scheme can be found in [14]. The infinite integrals in (32) and (33) are truncated at a certain large number N. Since all terms in (32) and (33) have the same property of the truncation error, the truncation error is symbolically estimated by the following integral.

$$Er = \int_N^\infty \sigma(\xi) G(x, \xi, y, 0)\mathrm{d}\xi, \tag{70}$$

where σ denotes one of components of the velocity vector defined by (31). When the truncation point $x = N$ is far from the field point (x, y), the asymptotic form of (70) is obtained.

$$Er \approx \frac{(1+\mathrm{i})K}{2\alpha_0 \Omega'(\alpha_0)}\sqrt{\frac{\pi}{\alpha_0}} \int_N^\infty \frac{\sigma(\xi)}{\sqrt{\xi}} \mathrm{e}^{-\mathrm{i}\alpha_0 \xi}\mathrm{d}\xi \approx \frac{(1-\mathrm{i})K}{2\alpha_0^2 \Omega'(\alpha_0)}\sqrt{\frac{\pi}{\alpha_0 N}} \mathrm{e}^{-\mathrm{i}\alpha_0 N}\sigma(N) = o(1/N), \tag{71}$$

where we have used the asymptotic behavior of the velocity vector, namely that $\sigma(x) = o(1/\sqrt{x})$ along the edge of the plate when $x \to \infty$ for the last reduction in (71). This result suggest that, if the truncation point N is large enough, the truncation error will be negligible for the following discussion.

Several numerical computations have been carried out to confirm the results obtained in the previous section. The input parameters for the computation are selected to simulate a trial design of an airport whose data are: 5,000 m in length and 1,500 m in width, 20 m as water depth, 6·0 s as design wave period, $8{\cdot}698 \times 10^{10}$ N m as flexural rigidity of the equivalent flat plate and 0·3 as Poisson's ratio. In this case, the wavelength in the water domain and in the plate estimated by the dispersion relation with the shallow approximation are 84·03 m and 222·20 m, respectively, while finite-depth theory gives a wavelength of 55·03 m and 218·05 m. The critical angle of the shallow-water approximation is 67·78°, while the exact value is 75·38°. The integral is truncated at $N = 20\pi/\alpha_0$ and the path of integration is divided into 256 segments.

As an example a typical result of $\varphi_1^{(2)}$ along the x-axis and y-axis is shown in Figure 2 on a logarithmic scale. In this case the angle of wave direction in the water domain χ equals 70° and that in the plate μ_{x0} equals 25·26°. It is apparent that the magnitude of $\varphi_1^{(2)}$ is proportional to $1/R$ as $R \to \infty$ and, near the truncation point, the truncation error appears. A wavy fluctuation appears on the curve at $x = 0$. The wave number of this fluctuation equals the y-component of the wave number in the water domain k_y. Thus, this fluctuation disappears inside the plate. The results suggest that $\vec{\varphi}_L$ is asymptotically proportional to $1/R$ as $R \to \infty$ on the x- and y-axis. Figure 3 shows the magnitude of $\varphi_1^{(2)}$ along the radial sections. It is clear that curves of the magnitude for $\beta = 75°$ and $\beta = 60°$ are proportional to $1/\sqrt{R}$ as $R \to \infty$. The decay of other curves is slower than $1/\sqrt{R}$ as $R \to \infty$. Especially, the decay of the curve for $\beta = 30^o$ is very slow, since this radial section is close to the line $\beta = \mu_{x0}$. These results confirm the asymptotic form of the solution as obtained in the previous section.

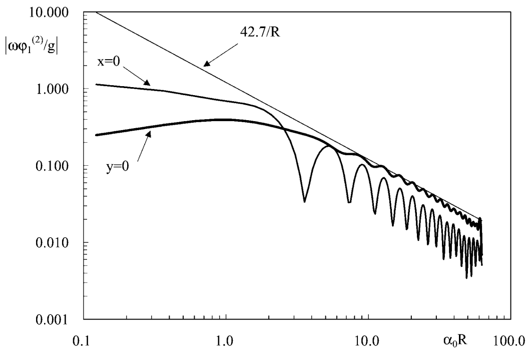

Figure 2. A typical numerical result of $\varphi_1^{(2)}$ along the x-axis and y-axis for $h = 20{\cdot}0$ m, $D = 8{\cdot}698 \times 10^{10}$ N m, $2\pi/\omega = 6{\cdot}0$ s and $\chi = 70°$.

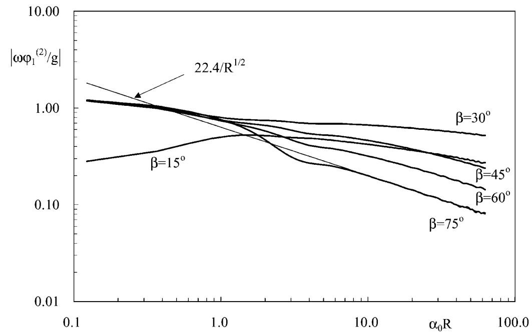

Figure 3. Magnitude of $\varphi_1^{(2)}$ along the radial sections for $h = 20{\cdot}0$ m, $D = 8{\cdot}698 \times 10^{10}$ N m, $2\pi/\omega = 6{\cdot}0$ s and $\chi = 70°$.

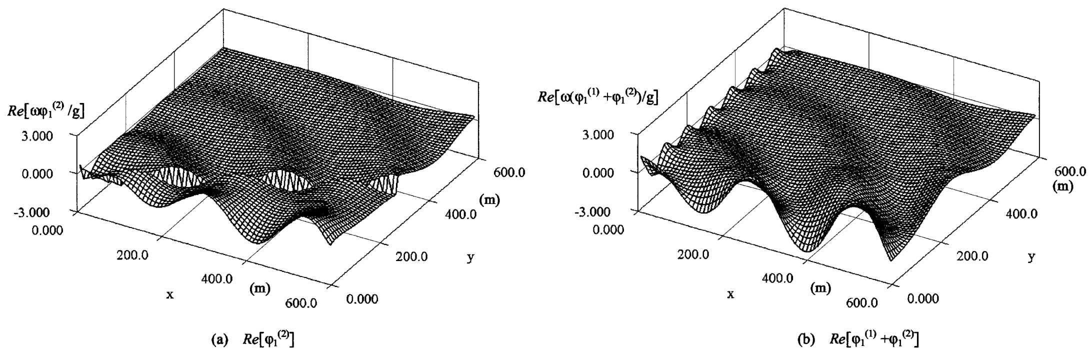

Figure 4. The three-dimensional plots of (a) $\Re\mathfrak{e}[\varphi_1^{(2)}]$ and (b) $\Re\mathfrak{e}[\varphi_1^{(1)} + \varphi_1^{(2)}]$ near the corner for $h = 20{\cdot}0$ m, $D = 8{\cdot}698 \times 10^{10}$ N m, $2\pi/\omega = 6{\cdot}0$ s and $\chi = 70°$.

The three-dimensional plot of $\Re\mathfrak{e}[\varphi_1^{(2)}]$ near the corner is shown in Figure 4a. The magnitude of $\varphi_1^{(2)}$ decays quickly along both edges. On the other hand, the decay of the magnitude is very slow along the line $\beta = \mu_{x0}$ and $\varphi_1^{(2)}$ is discontinuous along this line. Figure 4b shows the three-dimensional plot of $\Re\mathfrak{e}[\varphi_1^{(1)} + \varphi_1^{(2)}]$. The discontinuity line vanishes in this figure, since the discontinuity in $\varphi_1^{(2)}$ matches that in $\varphi_1^{(1)}$. Equation (54) implies that $\varphi_1^{(1)}$ has the other discontinuity along the line $\beta = \Re\mathfrak{e}[\mu_{x2}]$. However, this discontinuity is not visible in Figure 4a, since the magnitude of it is very small and it decays exponentially as R increases. Figure 4 also shows that the magnitude of $\varphi_1^{(2)}$ is small by comparison with that of $\varphi_1^{(1)}$, except for the domain near the line $\beta = \mu_{x0}$.

9. Conclusion

We have focused on the quarter-plane problem of a floating elastic plate to obtain a simple representation of the hydroelastic behavior of VLFS. We began by deriving a boundary-integral equation with a Green function, which satisfies the elastic free-surface condition. Averaging it in the vertical direction, we obtained the shallow-water approximation of the boundary-integral equation. Then, in order to decompose the solution into a simple form, the contribution of the half-plane problem for the integral equation was estimated.

We concluded that the following asymptotic behaviors characterize the solution of the quarter-plane problem. The end effect of the forcing term is asymptotically proportional to $1/\sqrt{R}$, except for the domain near the line $\beta = \mu_{x0}$. A similar result is also obtained in the water domain. The asymptotic form of the quarter-plane problem coincides with the solution of the half-plane problem far from the corner and the anti-symmetric-type parabolic approximation presents the asymptotic form near the line $\beta = \mu_{x0}$. If one moves the observation point closer to the corner, all other corner effects should be taken into account, since these terms are asymptotically proportional to $1/\sqrt{R}$. On both edges, these terms are still negligible, since they decay more rapidly than $1/\sqrt{R}$, *i.e.*, they are proportional to $1/R$, as was demonstrated numerically. Numerical results in Section 8 confirm the asymptotic form of the solution.

From a practical point of view, the solution of the half-plane problem $\varphi_1^{(1)}$ is a good approximation to represent the hydroelastic behavior of VLFS. The influence of $\varphi_1^{(2)}$ should be taken into account near the line $\beta = \mu_{x0}$; however, the anti-symmetric-type parabolic approximation gives a good approximation near this line. These calculations are not time-consuming and, therefore, they are suitable for the conceptual design stage of VLFS. If one wants to know the hydroelastic behavior more precisely, the estimation of $\varphi_1^{(2)}$ will be necessary. However, since the magnitude of $\varphi^{(2)}$ decays quickly near both the edges and the influence of it is limited around the corner, it may be ignorable in the conceptual design.

Appendix A, Half-plane problem

The procedure to solve the upper-half-plane problem and the right-half-plane problem is briefly described here for the convenience of the reader. The result of Evans and Davies [3] may be of help to know details of the theory, since their result is almost identical to that of the theory shown here.

The velocity potential of the upper-half-plane problem $\varphi_{U1}^{(1)}$ is composed of three terms in the plate as in (40). On the other hand, it is composed of incident waves and reflected waves in the water domain

$$\varphi_{U1}^{(1)} = \mathrm{e}^{-\mathrm{i}k_0(x\cos\chi + y\sin\chi)} + A_r\mathrm{e}^{-\mathrm{i}k_0(x\cos\chi - y\sin\chi)} \qquad \text{for} \quad y < 0, \tag{A1}$$

where A_r is the reflection coefficient of the upper-half-plane problem. The velocity potential $\varphi_{U1}^{(1)}$ satisfies the continuity of the potential and the flux at the edge of the plate. $\varphi_{U1}^{(1)}$ also satisfies two end conditions at the edge of the plate. The unknown coefficients A_n $(n = 0, 1, 2)$ and A_r are determined by solving these four equations simultaneously.

The velocity potential of the right-half-plane problem $\varphi_{R1}^{(1)}$ is represented as (42) in the plate. In the water domain, again the velocity potential $\varphi_{R1}^{(1)}$ is composed of incident waves and reflected waves

$$\varphi_{R1}^{(1)} = \mathrm{e}^{-\mathrm{i}k_0(x\cos\chi + y\sin\chi)} + C_r\mathrm{e}^{-\mathrm{i}k_0(-x\cos\chi + y\sin\chi)} \qquad \text{for} \quad x < 0, \tag{A2}$$

where C_r is the reflection coefficient of the right-half-plane problem. The unknown coefficients C_n and C_r are determined from the continuity conditions and the edge boundary conditions.

Appendix B, Asymptotic form of the forcing term

The sinusoidal distribution of the velocity at the edge of VLFS gives the following contribution to the boundary-integral equation

$$
\begin{aligned}
I &= \lim_{\epsilon,\iota\to 0}\frac{1}{2\pi}\int_0^\infty \mathrm{e}^{-\mathrm{i}(k_x-\mathrm{i}\epsilon)x'}\int_0^\infty \frac{K}{k}\left(\frac{1}{K-\mathrm{i}\iota-(1+Mk^4)k^2h}-\frac{1}{K-\mathrm{i}\iota}\right)J_0(kR')\mathrm{d}k\mathrm{d}x' \\
&= \lim_{\epsilon,\iota\to 0}\frac{-\mathrm{i}}{4\pi^2}\int_0^\infty \frac{K}{k}\left(\frac{1}{K-\mathrm{i}\iota-(1+Mk^4)k^2h}-\frac{1}{K-\mathrm{i}\iota}\right)\int_{-\pi+\beta}^{\pi+\beta}\frac{\mathrm{e}^{-\mathrm{i}kR\cos(\theta-\beta)}}{k_x-\mathrm{i}\epsilon-k\cos\theta}\mathrm{d}\theta\mathrm{d}k.
\end{aligned}
\tag{B1}
$$

When ϵ becomes infinitesimal, the second integral in Equation (B1) is singular. The singularity of this integral is removed by the contour integral

$$
\begin{aligned}
\lim_{\epsilon\to 0}\int_{-\pi+\beta}^{\pi+\beta}\frac{e^{-\mathrm{i}kR\cos(\theta-\beta)}}{k_x-\mathrm{i}\epsilon-k\cos\theta}\mathrm{d}\theta &= \mathrm{i}\int_{-\infty}^{\infty}\frac{\mathrm{e}^{-\mathrm{i}kR\cosh\theta}}{k_x-k\cos(\beta+\mathrm{i}\theta)}\mathrm{d}\theta-\mathrm{i}\int_{-\infty}^{\infty}\frac{\mathrm{e}^{\mathrm{i}kR\cosh\theta}}{k_x+k\cos(\beta+\mathrm{i}\theta)}\mathrm{d}\theta \\
&\quad +Cp_1+Cp_2.
\end{aligned}
\tag{B2}
$$

The path of integration is shown in Figure 5. According to β, the contributions from the poles are evaluated as

$$
Cp_1 = \begin{cases} 0 & \text{when } \theta_1 < \beta, \\ 2\pi\mathrm{i}\dfrac{\mathrm{e}^{-\mathrm{i}(k_x x+yk\sin\theta_1)}}{k\sin\theta_1} & \text{when } \theta_1 > \beta, \end{cases}
\tag{B3}
$$

$$
Cp_2 = -2\pi\mathrm{i}\frac{\mathrm{e}^{-\mathrm{i}(k_x x+yk\sin\theta_2)}}{k\sin\theta_2},
\tag{B4}
$$

where

$$
\theta_n = Cos^{-1}\frac{k_x}{k}, \qquad (\theta_1 > 0,\ \theta_2 < 0).
\tag{B5}
$$

The following two singular integrals are defined, and these integrals are altered by the contour integral with respect to k

$$
\begin{aligned}
I_1 &\equiv \lim_{\iota\to 0}\mathrm{i}\int_0^\infty \frac{K}{k}\left(\frac{1}{K-\mathrm{i}\iota-(1+Mk^4)k^2h}-\frac{1}{K-\mathrm{i}\iota}\right)\int_{-\infty}^{\infty}\frac{\mathrm{e}^{-\mathrm{i}kR\cosh\theta}}{k_x-k\cos(\beta+\mathrm{i}\theta)}\mathrm{d}k\mathrm{d}\theta \\
&= \mathrm{i}\int_0^\infty \frac{1}{k}\left(\frac{K}{K+(1+Mk^4)k^2h}-1\right)\int_{-\infty}^{\infty}\frac{\mathrm{e}^{-kR\cosh\theta}}{k_x+\mathrm{i}k\cos(\beta+\mathrm{i}\theta)}\mathrm{d}k\mathrm{d}\theta \\
&\quad +\frac{2\pi K}{\alpha_0\Omega'(\alpha_0)}\int_{-\infty}^{\infty}\frac{\mathrm{e}^{-\mathrm{i}\alpha_0 R\cosh\theta}}{k_x-\alpha_0\cos(\beta+\mathrm{i}\theta)}\mathrm{d}\theta+\frac{2\pi K}{\alpha_2\Omega'(\alpha_2)}\int_{-\infty}^{\infty}\frac{\mathrm{e}^{-\mathrm{i}\alpha_2 R\cosh\theta}}{k_x-\alpha_2\cos(\beta+\mathrm{i}\theta)}\mathrm{d}\theta \\
&\quad -2\pi\mathrm{e}^{-\mathrm{i}k_x x}\int_{-\infty}^{0}\frac{1}{k_x}\left(\frac{K}{K-\left(1+M\frac{k_x^4}{\cos^4(\beta+\mathrm{i}\theta)}\right)\frac{k_x^2h}{\cos^2(\beta+\mathrm{i}\theta)}}-1\right)\mathrm{e}^{-\mathrm{i}yk_x\tan(\beta+\mathrm{i}\theta)}\mathrm{d}\theta.
\end{aligned}
\tag{B6}
$$

$$
\begin{aligned}
I_2 &\equiv -\lim_{\iota\to 0}\mathrm{i}\int_0^\infty \frac{K}{k}\left(\frac{1}{K-\mathrm{i}\iota-(1+Mk^4)k^2h}-\frac{1}{K-\mathrm{i}\iota}\right)\int_{-\infty}^{\infty}\frac{\mathrm{e}^{\mathrm{i}kR\cosh\theta}}{k_x+k\cos(\beta+\mathrm{i}\theta)}\mathrm{d}k\mathrm{d}\theta \\
&= -\mathrm{i}\int_0^\infty \frac{1}{k}\left(\frac{K}{K+(1+Mk^4)k^2h}-1\right)\int_{-\infty}^{\infty}\frac{\mathrm{e}^{-kR\cosh\theta}}{k_x+\mathrm{i}k\cos(\beta+\mathrm{i}\theta)}\mathrm{d}k\mathrm{d}\theta \\
&\quad +\frac{2\pi K}{\alpha_1\Omega'(\alpha_1)}\int_{-\infty}^{\infty}\frac{\mathrm{e}^{\mathrm{i}\alpha_1 R\cosh\theta}}{k_x+\alpha_1\cos(\beta+\mathrm{i}\theta)}\mathrm{d}\theta.
\end{aligned}
\tag{B7}
$$

The last term of equation (B6) can be simplified as

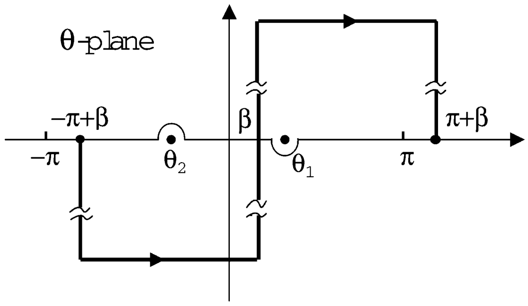

Figure 5. The path of integration for the contour integral of (B2).

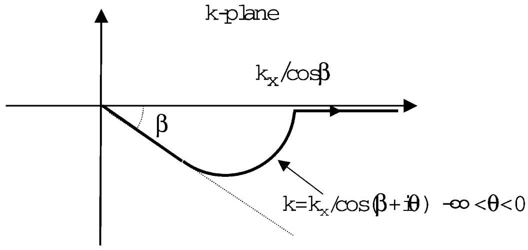

Figure 6. The path of integration for the integral (B8).

$$
\begin{aligned}
I_3 &\equiv -2\pi \mathrm{e}^{-\mathrm{i}k_x x} \int_{-\infty}^{0} \frac{1}{k_x} \left(\frac{K}{K - \left(1 + M\frac{k_x^4}{\cos^4(\beta+\mathrm{i}\theta)}\right)\frac{k_x^2 h}{\cos^2(\beta+\mathrm{i}\theta)}} - 1 \right) \mathrm{e}^{-\mathrm{i}yk_x \tan(\beta+\mathrm{i}\theta)} \mathrm{d}\theta \\
&= 2\pi \mathrm{i} \mathrm{e}^{-\mathrm{i}k_x x} \int_0^{\frac{k_x}{\cos\beta}} \frac{1}{k} \left(\frac{K}{K - \left(1 + Mk^4\right)k^2 h} - 1 \right) \frac{\mathrm{e}^{-\mathrm{i}y\sqrt{k^2-k_x^2}}}{\sqrt{k^2 - k_x^2}} \mathrm{d}k,
\end{aligned} \tag{B8}
$$

where the path of integration is shown in Figure 6.

Combining this integral with the contribution of C_{p1}, we derive the following equation. This integral is easily altered by the contour integral

$$
\begin{aligned}
&\frac{-\mathrm{i}}{4\pi^2} \left(I_3 + \int_{\frac{k_x}{\cos\beta}}^{\infty} \frac{1}{k} \left(\frac{K}{K - \left(1 + Mk^4\right)k^2 h} - 1 \right) C_{p1} \mathrm{d}k \right) \\
&\quad = \frac{1}{2\pi} \mathrm{e}^{-\mathrm{i}k_x x} \int_0^{\infty} \frac{1}{k} \left(\frac{K}{K - \left(1 + Mk^4\right)k^2 h} - 1 \right) \frac{\mathrm{e}^{-\mathrm{i}y\sqrt{k^2-k_x^2}}}{\sqrt{k^2 - k_x^2}} \mathrm{d}k \\
&\quad = \frac{1}{2\pi} \mathrm{e}^{-\mathrm{i}k_x x} \int_0^{\infty} \frac{1}{k} \left(\frac{K}{K + \left(1 + Mk^4\right)k^2 h} - 1 \right) \frac{\mathrm{e}^{-y\sqrt{k^2+k_x^2}}}{\sqrt{k^2 + k_x^2}} \mathrm{d}k + C_{I1} + C_{I3}.
\end{aligned} \tag{B9}
$$

Similarly the contribution of C_{p2} is evaluated as

$$
\begin{aligned}
&-\lim_{\iota\to 0} \frac{\mathrm{i}}{4\pi^2} \int_0^{\infty} \frac{K}{k} \left(\frac{1}{K - \mathrm{i}\iota\left(1 + Mk^4\right)k^2 h} - \frac{1}{K - \mathrm{i}\iota} \right) C_{p2} \mathrm{d}k \\
&\quad = \frac{1}{2\pi} e^{-\mathrm{i}k_x x} \int_0^{\infty} \frac{1}{k} \left(\frac{K}{K - \left(1 + Mk^4\right)k^2 h} - 1 \right) \frac{\mathrm{e}^{\mathrm{i}y\sqrt{k^2-k_x^2}}}{\sqrt{k^2 - k_x^2}} \mathrm{d}k \\
&\quad = -\frac{\mathrm{i}}{2\pi} \mathrm{e}^{-\mathrm{i}k_x x} \int_0^{\infty} \frac{1}{k} \left(\frac{K}{K + \left(1 + Mk^4\right)k^2 h} - 1 \right) \frac{\mathrm{e}^{-y\sqrt{k^2+k_x^2}}}{\sqrt{k^2 + k_x^2}} \mathrm{d}k + C_{I2}.
\end{aligned} \tag{B10}
$$

Summarizing these results, we represent the double integral I by the following single integrals

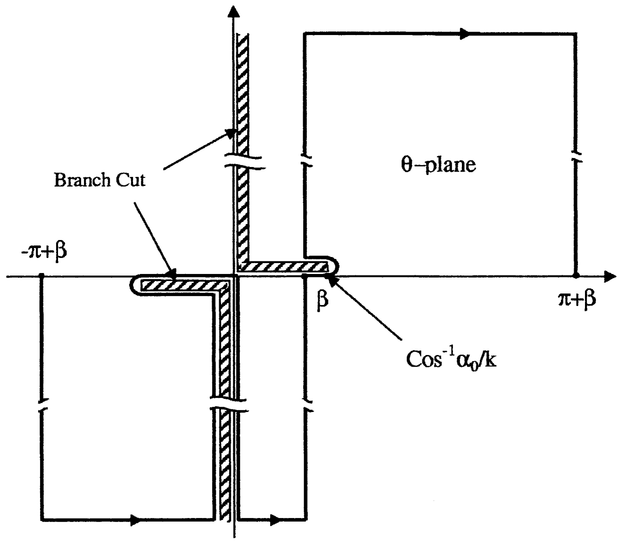

Figure 7. The path of integration for the contour integral of (C1).

$$\begin{aligned} I &= -\frac{\mathrm{i}}{4\pi^2}(I_1+I_2) - \lim_{\iota\to 0} -\frac{\mathrm{i}}{4\pi^2}\int_0^\infty \frac{K}{k}\left(\frac{1}{K-\mathrm{i}\iota\left(1+Mk^4\right)k^2h} - \frac{1}{K-\mathrm{i}\iota}\right)(C_{p1}+C_{p2})\mathrm{d}k \\ &= -\frac{\mathrm{i}}{2\pi}\frac{K}{\alpha_0\Omega'(\alpha_0)}\int_{-\infty}^{\infty}\frac{\mathrm{e}^{-\mathrm{i}\alpha_0 R\cosh\theta}}{k_x-\alpha_0\cos(\beta+\mathrm{i}\theta)}\mathrm{d}\theta - \frac{\mathrm{i}}{2\pi}\frac{K}{\alpha_1\Omega'(\alpha_1)}\int_{-\infty}^{\infty}\frac{\mathrm{e}^{\mathrm{i}\alpha_1 R\cosh\theta}}{k_x+\alpha_1\cos(\beta+\mathrm{i}\theta)}\mathrm{d}\theta \qquad \text{(B11)} \\ &\quad -\frac{\mathrm{i}}{2\pi}\frac{K}{\alpha_2\Omega'(\alpha_2)}\int_{-\infty}^{\infty}\frac{\mathrm{e}^{-\mathrm{i}\alpha_2 R\cosh\theta}}{k_x-\alpha_2\cos(\beta+\mathrm{i}\theta)}\mathrm{d}\theta + C_{I1}+C_{I2}+C_{I3}. \end{aligned}$$

When R approaches infinity, the stationary-phase method is applied and the asymptotic form of the integral I is obtained:

$$I \sim -\frac{2}{\pi}\frac{K}{\alpha_0\sqrt{\pi}\Omega'(\alpha_0)}\frac{\mathrm{e}^{-\mathrm{i}\alpha_0 R+\mathrm{i}\frac{\pi}{4}}}{(k_x-\alpha_0\cos\beta)\sqrt{R}} + C_{I1}+C_{I2}+C_{I3}. \qquad \text{(B12)}$$

Appendix C, Asymptotic form of $\vec{\varphi}_R$

In order to estimate the influence due to the term which is proportional to $1/\sqrt{R}$, the following integral is performed

$$\begin{aligned} I_s &= \lim_{\epsilon,\iota\to 0}\frac{1}{2\pi}\int_0^\infty \frac{1}{\sqrt{x'}}\mathrm{e}^{-\mathrm{i}(\alpha_o-\mathrm{i}\epsilon)x'}\int_0^\infty\frac{K}{k}\left(\frac{1}{K-\mathrm{i}\iota-(1+Mk^4)k^2h}-\frac{1}{K-\mathrm{i}\iota}\right)J_0(kR')\mathrm{d}k\mathrm{d}x' \\ &= \lim_{\epsilon,\iota\to 0}\frac{1}{4\pi\sqrt{\pi}}\mathrm{e}^{-\frac{\pi}{4}\mathrm{i}}\int_0^\infty\frac{K}{k}\left(\frac{1}{K-\mathrm{i}\iota-(1+Mk^4)k^2h}-\frac{1}{K-\mathrm{i}\iota}\right)\times \qquad \text{(C1)} \\ &\quad \times\int_{-\pi+\beta}^{\pi+\beta}\frac{\mathrm{e}^{-\mathrm{i}kR\cos(\theta-\beta)}}{\sqrt{\alpha_0-\mathrm{i}\epsilon-k\cos\theta}}\mathrm{d}\theta, \end{aligned}$$

where ϵ determines the shapes of the branch cut shown in Figure 7. The evaluation of this integral is described in this appendix.

The path of the integral and the branch cut of the second integral of (C1) are depicted in Figure 7. This integral is altered by the contour integral

$$\lim_{\epsilon\to 0}\int_{-\pi+\beta}^{\pi+\beta}\frac{\mathrm{e}^{-\mathrm{i}kR\cos(\theta-\beta)}}{\sqrt{\alpha_0-\mathrm{i}\epsilon-k\cos\theta}}\mathrm{d}\theta = 2\mathrm{i}\int_0^{-\cos^{-1}\frac{\alpha_0}{k}}\frac{\mathrm{e}^{-\mathrm{i}kR\cos(\theta-\beta)}}{\sqrt{k\cos\theta-\alpha_0}}d\theta + 2\mathrm{i}\int_{\cos^{-1}\frac{\alpha_0}{k}}^{\beta}\frac{\mathrm{e}^{-\mathrm{i}kR\cos(\theta-\beta)}}{\sqrt{k\cos\theta-\alpha_0}}\mathrm{d}\theta$$
$$+\mathrm{i}\lim_{\epsilon\to 0}\int_0^{\infty}\frac{\mathrm{e}^{-\mathrm{i}kR\cos(\beta+\mathrm{i}\theta)}}{\sqrt{\alpha_0-k\cosh\theta+\mathrm{i}\epsilon}}\mathrm{d}\theta - \mathrm{i}\lim_{\epsilon\to 0}\int_0^{\infty}\frac{\mathrm{e}^{-\mathrm{i}kR\cos(\beta+\mathrm{i}\theta)}}{\sqrt{\alpha_0-k\cosh\theta-\mathrm{i}\epsilon}}\mathrm{d}\theta \quad \text{(C2)}$$
$$+\mathrm{i}\int_{-\infty}^{\infty}\frac{\mathrm{e}^{-\mathrm{i}kR\cosh\theta}}{\sqrt{\alpha_0-k\cos(\beta+\mathrm{i}\theta)}}\mathrm{d}\theta - \mathrm{i}\int_{-\infty}^{\infty}\frac{\mathrm{e}^{\mathrm{i}kR\cosh\theta}}{\sqrt{\alpha_0+k\cos(\beta+\mathrm{i}\theta)}}\mathrm{d}\theta.$$

The following two singular integrals are defined, and these integrals are altered by the contour integral respect to k

$$I_4 \equiv \lim_{\iota\to 0}\mathrm{i}\int_0^{\infty}\frac{K}{k}\left(\frac{1}{K-\mathrm{i}\iota-(1+Mk^4)k^2h}-\frac{1}{K-\mathrm{i}\iota}\right)\int_{-\infty}^{\infty}\frac{\mathrm{e}^{-\mathrm{i}kR\cosh\theta}}{\sqrt{\alpha_0-k\cos(\beta+\mathrm{i}\theta)}}\mathrm{d}k\mathrm{d}\theta$$
$$= \mathrm{i}\int_0^{\infty}\frac{1}{k}\left(\frac{K}{K+(1+Mk^4)k^2h}-1\right)\int_{-\infty}^{\infty}\frac{\mathrm{e}^{-kR\cosh\theta}}{\sqrt{\alpha_0+\mathrm{i}k\cos(\beta+\mathrm{i}\theta)}}\mathrm{d}k\mathrm{d}\theta$$
$$+\frac{2\pi K}{\alpha_0\Omega'(\alpha_0)}\int_{-\infty}^{\infty}\frac{\mathrm{e}^{-\mathrm{i}\alpha_0R\cosh\theta}}{\sqrt{\alpha_0-\alpha_0\cos(\beta+\mathrm{i}\theta)}}\mathrm{d}\theta + \frac{2\pi K}{\alpha_2\Omega'(\alpha_2)}\int_{-\infty}^{\infty}\frac{\mathrm{e}^{-\mathrm{i}\alpha_2R\cosh\theta}}{\sqrt{\alpha_0-\alpha_2\cos(\beta+\mathrm{i}\theta)}}\mathrm{d}\theta \quad \text{(C3)}$$
$$+2\mathrm{i}\int_{\alpha_0}^{\infty}\frac{\mathrm{e}^{-\mathrm{i}xs}}{\sqrt{s-\alpha_0}}\int_0^{\frac{s}{\cos\beta}}\frac{1}{k}\left(\frac{K}{K-(1+Mk^4)k^2h}-1\right)\frac{\mathrm{e}^{-\mathrm{i}y\sqrt{k^2-s^2}}}{\sqrt{k^2-s^2}}\mathrm{d}k\mathrm{d}s.$$

$$I_5 \equiv -\lim_{\iota\to 0}\mathrm{i}\int_0^{\infty}\frac{K}{k}\left(\frac{1}{K-\mathrm{i}\iota-(1+Mk^4)k^2h}-\frac{1}{K-\mathrm{i}\iota}\right)\int_{-\infty}^{\infty}\frac{\mathrm{e}^{\mathrm{i}kR\cosh\theta}}{\sqrt{\alpha_0+k\cos(\beta+\mathrm{i}\theta)}}\mathrm{d}k\mathrm{d}\theta$$
$$= -\mathrm{i}\int_0^{\infty}\frac{1}{k}\left(\frac{K}{K+(1+Mk^4)k^2h}-1\right)\int_{-\infty}^{\infty}\frac{\mathrm{e}^{-kR\cosh\theta}}{\sqrt{\alpha_0+\mathrm{i}k\cos(\beta+\mathrm{i}\theta)}}\mathrm{d}k\mathrm{d}\theta \quad \text{(C4)}$$
$$+\frac{2\pi K}{\alpha_1\Omega'(\alpha_1)}\int_{-\infty}^{\infty}\frac{\mathrm{e}^{\mathrm{i}\alpha_1R\cosh\theta}}{\sqrt{\alpha_0+\alpha_1\cos(\beta+\mathrm{i}\theta)}}\mathrm{d}\theta.$$

When the integral I_4 is altered, the contour integral is applied and its integral path is depicted in Figure 8. In this figure the branch cut of $\sqrt{\alpha_0-k\cos(\beta+\mathrm{i}\theta)}$ is also depicted. It is noted that the integral path of the last term of Equation (C3) is not on the real axis and this path is indicated in Figure 8.

The third and fourth term of Equation (C3) give the following integral and it is altered by the contour integral

$$I_6 \equiv -\lim_{\iota,\epsilon\to 0}\mathrm{i}\int_0^{\infty}\frac{K}{k}\left(\frac{1}{K-\mathrm{i}\iota-(1+Mk^4)k^2h}-\frac{1}{K-\mathrm{i}\iota}\right)\left[\int_0^{\infty}\frac{\mathrm{e}^{-\mathrm{i}kR\cos(\beta+\mathrm{i}\theta)}}{\sqrt{\alpha_0-k\cosh\theta+\mathrm{i}\epsilon}}\,\mathrm{d}\theta\right.$$
$$\left.-\int_0^{\infty}\frac{\mathrm{e}^{-\mathrm{i}kR\cos(\beta+i\theta)}}{\sqrt{\alpha_0-k\cosh\theta-\mathrm{i}\epsilon}}\mathrm{d}\theta\right] = 2\mathrm{i}\int_{\alpha_0}^{\infty}\frac{\mathrm{e}^{-\mathrm{i}xs}}{\sqrt{s-\alpha_0}}\int_0^{s}\frac{1}{k}\left(\frac{K}{K-(1+Mk^4)k^2h}-1\right)\frac{\mathrm{e}^{\mathrm{i}y\sqrt{k^2-s^2}}}{\sqrt{k^2-s^2}}\mathrm{d}k\mathrm{d}s. \quad \text{(C5)}$$

Combining the last term of Equation (C3) with the contribution from the second term of Equation (C2), we derive the following equation. This integral is easily altered by the contour integral

$$I_7 \equiv 2\mathrm{i}\int_{\frac{\alpha_0}{\cos\beta}}^{\infty}\frac{1}{k}\left(\frac{K}{K+(1+Mk^4)k^2h}-1\right)\int_{\cos^{-1}\frac{\alpha_0}{k}}^{\beta}\frac{\mathrm{e}^{-\mathrm{i}kR\cos(\theta-\beta)}}{\sqrt{k\cos\theta-\alpha_0}}\mathrm{d}\theta dk$$
$$= 2\mathrm{i}\int_{\alpha_0}^{\infty}\frac{\mathrm{e}^{-\mathrm{i}xs}}{\sqrt{s-\alpha_0}}\int_{\frac{s}{\cos\beta}}^{\infty}\frac{1}{k}\left(\frac{K}{K-(1+Mk^4)k^2h}-1\right)\frac{\mathrm{e}^{-\mathrm{i}y\sqrt{k^2-s^2}}}{\sqrt{k^2-s^2}}\mathrm{d}k\mathrm{d}s. \quad \text{(C6)}$$

Similarly the contribution of the first term is evaluated as

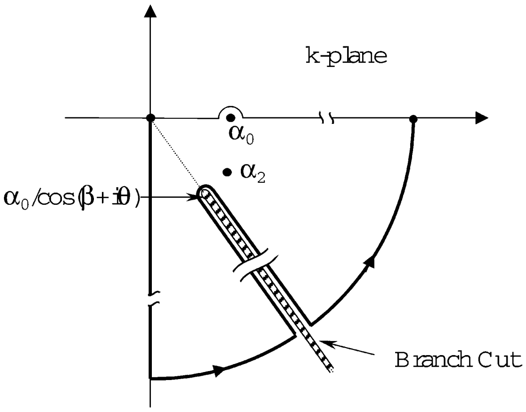

Figure 8. The path of integration for the contour integral of (C4).

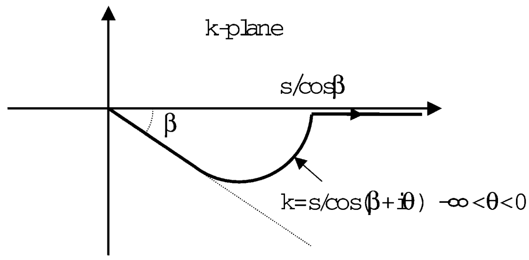

Figure 9. The path of integration for the integral (C3).

$$
\begin{aligned}
I_8 \ &\equiv -2\mathrm{i}\int_{\alpha_0}^{\infty}\frac{1}{k}\left(\frac{K}{K-(1+Mk^4)k^2h}-1\right)\int_{\cos^{-1}\frac{\alpha_0}{k}}^{0}\frac{\mathrm{e}^{-\mathrm{i}kR\cos(\theta-\beta)}}{\sqrt{k\cos\theta-\alpha_0}}\mathrm{d}\theta\mathrm{d}k \\
&= 2\mathrm{i}\int_{\alpha_0}^{\infty}\frac{\mathrm{e}^{-\mathrm{i}xs}}{\sqrt{s-\alpha_0}}\int_{s}^{\infty}\frac{1}{k}\left(\frac{K}{K-(1+Mk^4)k^2h}-1\right)\frac{\mathrm{e}^{\mathrm{i}y\sqrt{k^2-s^2}}}{\sqrt{k^2-s^2}}\mathrm{d}k\mathrm{d}s.
\end{aligned}
\tag{C7}
$$

Adding integral I_8 to I_6, we obtain the following intgral and it is altered by the contour integral

$$
\begin{aligned}
I_6+I_8 = 2\int_{\alpha_0}^{\infty}\frac{\mathrm{e}^{-\mathrm{i}xs}}{\sqrt{s-\alpha_0}}\int_{0}^{\infty}\frac{1}{k}\left(\frac{K}{K+(1+Mk^4)k^2h}-1\right)\frac{\mathrm{e}^{-y\sqrt{k^2+k_x^2}}}{\sqrt{k^2+k_x^2}}\mathrm{d}k\mathrm{d}s \\
-\frac{4\pi K}{\alpha_1\Omega'(\alpha_1)}\int_{\alpha_0}^{\infty}\frac{\mathrm{e}^{-\mathrm{i}xs+\mathrm{i}y\sqrt{\alpha_1^2-s^2}}}{\sqrt{s-\alpha_0}\sqrt{\alpha_1^2-s^2}}\mathrm{d}s.
\end{aligned}
\tag{C8}
$$

Similarly, the following integral is obtained from I_7 and the last term of I_4, namely

$$
\begin{aligned}
\text{The last term of} I_4+I_7 = -2\int_{\alpha_0}^{\infty}\frac{\mathrm{e}^{-\mathrm{i}xs}}{\sqrt{s-\alpha_0}}\int_{0}^{\infty}\frac{1}{k}\left(\frac{K}{K+(1+Mk^4)k^2h}-1\right)\frac{\mathrm{e}^{-y\sqrt{k^2+s^2}}}{\sqrt{k^2+s^2}}\mathrm{d}k\mathrm{d}s \\
+\frac{2\pi K}{\alpha_2\Omega'(\alpha_2)}\int_{\alpha_0}^{\alpha_2'}\frac{\mathrm{e}^{-\mathrm{i}xs-\mathrm{i}y\sqrt{\alpha_2^2-s^2}}}{\sqrt{s-\alpha_0}\sqrt{\alpha_2^2-s^2}}\mathrm{d}s,
\end{aligned}
\tag{C9}
$$

where $(\alpha_2', 0)$ is a cross point between $\alpha_2\cos(\beta+\mathrm{i}\theta)$ $(-\infty<\theta<\infty)$ and the real axis and, therefore, if arg$[\alpha_2]$ is smaller than β, α_2' would be infinity.

Summarizing these results, the double integral I_s is represented by the single integrals

$$
\begin{aligned}
I_s = & \int_0^\infty \frac{1}{\sqrt{x'}} \mathrm{e}^{-\mathrm{i}\alpha_0 x'} G(x,y,x',0)\mathrm{d}x' = \frac{K(1-\mathrm{i})}{2\sqrt{2\pi}\alpha_0\Omega'(\alpha_0)} \int_{-\infty}^\infty \frac{\mathrm{e}^{-\mathrm{i}\alpha_0 R\cosh\theta}}{\sqrt{\alpha_0-\alpha_0\cos(\beta+\mathrm{i}\theta)}}\mathrm{d}\theta \\
& + \frac{K(1-\mathrm{i})}{2\sqrt{2\pi}\alpha_1\Omega'(\alpha_1)} \int_{-\infty}^\infty \frac{\mathrm{e}^{\mathrm{i}\alpha_1 R\cosh\theta}}{\sqrt{\alpha_0+\alpha_1\cos(\beta+\mathrm{i}\theta)}}\mathrm{d}\theta \\
& + \frac{K(1-\mathrm{i})}{2\sqrt{2\pi}\alpha_2\Omega'(\alpha_2)} \int_{-\infty}^\infty \frac{\mathrm{e}^{-\mathrm{i}\alpha_2 R\cosh\theta}}{\sqrt{\alpha_0-\alpha_2\cos(\beta+\mathrm{i}\theta)}}\mathrm{d}\theta \\
& - \frac{K(1-\mathrm{i})}{\sqrt{2\pi}\alpha_1\Omega'(\alpha_1)} \int_{\alpha_0}^\infty \frac{\mathrm{e}^{-\mathrm{i}xs+\mathrm{i}y\sqrt{\alpha_1^2-s^2}}}{\sqrt{s-\alpha_0}\sqrt{\alpha_1^2-s^2}}\mathrm{d}s + \frac{K(1-\mathrm{i})}{\sqrt{2\pi}\alpha_2\Omega'(\alpha_2)} \int_{\alpha_0}^{\alpha_2'} \frac{\mathrm{e}^{-\mathrm{i}xs-\mathrm{i}y\sqrt{\alpha_2^2-s^2}}}{\sqrt{s-\alpha_0}\sqrt{\alpha_2^2-s^2}}\mathrm{d}s.
\end{aligned}
\tag{C10}
$$

The asymptotic form of I_s is obtained by employing the stationary-phase method

$$
\begin{aligned}
I_s \sim & -\mathrm{i}\frac{K}{\sqrt{2}\alpha_0^2\Omega'(\alpha_0)} \frac{\mathrm{e}^{-\mathrm{i}\alpha_0 R}}{\sqrt{1-\cos\beta}}\sqrt{\frac{1}{R}} + \mathrm{i}\frac{2K}{\alpha_1\sqrt{\alpha_1^2-\alpha_0^2}\Omega'(\alpha_1)} \frac{\mathrm{e}^{-\mathrm{i}x\alpha_0+\mathrm{i}y\sqrt{\alpha_1^2-\alpha_0^2}}}{\sqrt{x}} \\
& -\mathrm{i}\frac{2K}{\alpha_2\sqrt{\alpha_2^2-\alpha_0^2}\Omega'(\alpha_2)} \frac{\mathrm{e}^{-\mathrm{i}x\alpha_0-\mathrm{i}y\sqrt{\alpha_2^2-\alpha_0^2}}}{\sqrt{x}}.
\end{aligned}
\tag{C11}
$$

In order to estimate the influence of the term whose magnitude is proportional to $1/\sqrt{R}$ and wave number is k_0, we perform the following integral and evaluate the asymptotic form with the same procedure. The result is

$$
\begin{aligned}
& \int_0^\infty \frac{1}{\sqrt{x'}} \mathrm{e}^{-\mathrm{i}k_0 x'} G(x,y,x',0)\mathrm{d}x' = \frac{K(1-\mathrm{i})}{2\sqrt{2\pi}\alpha_0\Omega'(\alpha_0)} \int_{-\infty}^\infty \frac{\mathrm{e}^{-\mathrm{i}\alpha_0 R\cosh\theta}}{\sqrt{k_0-\alpha_0\cos(\beta+\mathrm{i}\theta)}}\mathrm{d}\theta \\
& + \frac{K(1-\mathrm{i})}{2\sqrt{2\pi}\alpha_1\Omega'(\alpha_1)} \int_{-\infty}^\infty \frac{\mathrm{e}^{\mathrm{i}\alpha_1 R\cosh\theta}}{\sqrt{k_0+\alpha_1\cos(\beta+\mathrm{i}\theta)}}\mathrm{d}\theta \\
& + \frac{K(1-\mathrm{i})}{2\sqrt{2\pi}\alpha_2\Omega'(\alpha_2)} \int_{-\infty}^\infty \frac{\mathrm{e}^{-\mathrm{i}\alpha_2 R\cosh\theta}}{\sqrt{k_0-\alpha_2\cos(\beta+\mathrm{i}\theta)}}\mathrm{d}\theta \\
& - \frac{K(1-\mathrm{i})}{\sqrt{2\pi}\alpha_1\Omega'(\alpha_1)} \int_{k_0}^\infty \frac{\mathrm{e}^{-\mathrm{i}xs+\mathrm{i}y\sqrt{\alpha_1^2-s^2}}}{\sqrt{s-k_0}\sqrt{\alpha_1^2-s^2}}\mathrm{d}s + \frac{K(1-\mathrm{i})}{\sqrt{2\pi}\alpha_2\Omega'(\alpha_2)} \int_{k_0}^{\alpha_2'} \frac{\mathrm{e}^{-\mathrm{i}xs-\mathrm{i}y\sqrt{\alpha_2^2-s^2}}}{\sqrt{s-k_0}\sqrt{\alpha_2^2-s^2}}\mathrm{d}s \\
& \sim -\mathrm{i}\frac{K}{\sqrt{2}\alpha_0\sqrt{\alpha_0}\Omega'(\alpha_0)} \frac{\mathrm{e}^{-\mathrm{i}\alpha_0 R}}{\sqrt{k_0-\alpha_0\cos\beta}}\sqrt{\frac{1}{R}} + \mathrm{i}\frac{2K}{\alpha_1\sqrt{\alpha_1^2-k_0^2}\Omega'(\alpha_1)} \frac{\mathrm{e}^{-\mathrm{i}xk_0+\mathrm{i}y\sqrt{\alpha_1^2-k_0^2}}}{\sqrt{x}} \\
& -\mathrm{i}\frac{2K}{\alpha_2\sqrt{\alpha_2^2-k_0^2}\Omega'(\alpha_2)} \frac{\mathrm{e}^{-\mathrm{i}xk_0-\mathrm{i}y\sqrt{\alpha_2^2-k_0^2}}}{\sqrt{x}}.
\end{aligned}
\tag{C12}
$$

In order to know the asymptotic form in the water domain, we perform the following integral and evaluate the asymptotic form

$$\int_0^\infty \frac{1}{\sqrt{x'}} e^{-i\alpha_0 x'} G_w(x, y, x', 0) dx' = -\frac{(1-i)}{4\sqrt{2\pi}} \int_{-\infty}^{\infty} \frac{e^{-ik_0 R \cosh\theta}}{\sqrt{\alpha_0 - k_0 \cos(\beta + i\theta)}} d\theta$$

$$-\frac{(1-i)}{2\sqrt{2\pi}} \int_{\alpha_0}^{k_0 \cos\beta} \frac{e^{-ixs + iy\sqrt{k_0^2 - s^2}}}{\sqrt{s - \alpha_0}\sqrt{k_0^2 - s^2}} ds$$

$$\sim \begin{cases} i\dfrac{2\sqrt{k_0}}{\sqrt{k_0^2 - \alpha_0^2}} \dfrac{e^{-ix\alpha_0 + iy\sqrt{k_0^2 - \alpha_0^2}}}{\sqrt{x + y\frac{\alpha_0}{\sqrt{k_0^2 - \alpha_0^2}}}} - \dfrac{1}{2\sqrt{2k_0}} \dfrac{e^{-ik_0 R}}{\sqrt{k_0 \cos\beta - \alpha_0}} \sqrt{\dfrac{1}{R}} & \text{when} \quad -\beta_c < \beta < 0, \\ i\dfrac{1}{2\sqrt{2k_0}} \dfrac{e^{-ik_0 R}}{\sqrt{\alpha_0 - k_0 \cos\beta}} \sqrt{\dfrac{1}{R}} & \text{when} \quad -\frac{3}{2}\pi < \beta < -\beta_c, \end{cases} \quad \text{(C13, C14)}$$

where

$$\beta_c = \left| \arctan \frac{\alpha_0}{k_0} \right|.$$

Acknowledgement

It is acknowledged that a part of this work was done while the author was staying at the University of Bristol. The author is grateful to Professor David Evans for valuable discussions.

References

1. M. Ohkusu and Y. Nanba, Analysis of hydroelastic behavior of a large floating platform of thin plate configuration in waves. *Proceedings of Int. Workshop on VLFS, Hayama, Japan* (1996) 143–148.
2. J.J. Stoker, *Water Waves*. New York: Inter-science (1957) 567pp.
3. D.V. Evans and T.V. Davies, *Wave-Ice Interaction*. Technical report.1313, Davidson Lab., Stevens Inst. of Techno., Hoboken, N.J. (1968) 102pp.
4. C. Fox and V.A. Squire, Reflection and transmission characteristics at the edge of shore fast sea ice. *J. Geophys. Res.* 95 (1990) 11629–11639.
5. M. Meylan and V.A. Squire, Finite-floe wave reflection and transmission coefficient from a semi-infinite model. *J. Geophys. Res.* 98 (1993) 12537–12542.
6. M. Meylan and V.A. Squire, Response of a circular ice floe to ocean waves. *J. Geophys. Res.* 101 (1996) 8869–8884.
7. G. Zilman and T. Miloh, Hydroelastic buoyant circular plate in shallow water: a closed form solution. *Appl. Ocean Res.* 22 (2000) 191–198.
8. J.W. Kim and R.C. Ertekin, An eigenfunction-expansion method for predicting hydroelastic behavior of a shallow-draft VLFS. In: M. Kashiwagi *et al*. (eds.), *Hydroelasticity in Marine Technology*. RIAM Kyushu University (1998) pp. 47–59.
9. S.P. Timoshenko and J.M. Gere, *Theory of Elastic Stability*. New York: McGraw-Hill (1961) 541 pp.
10. F. John, On the motion of floating bodies II. *Comm. Pure Appl. Math.* 3 (1950) 45–101.
11. A.J. Hermans, A boundary element method for the interaction of free-surface waves with a very large floating flexible platform. *J. Fluids Struct.* 14 (2000) 943–956.
12. K. Takagi, Hydroelastic response of a very large floating structure in waves -a simple representation by the parabolic approximation. *Appl. Ocean Res.* 24 (2002) 175–183.
13. C.C. Mei, *Applied Ocean Waves*. Singapore: World Science Publishing (1989) 740pp.
14. R.C. Ertekin and J.W. Kim, Hydroelastic response of a floating mat-type structure in oblique shallow-water waves. *J. Ship Res.* 43 (1999) 241–254.